

1 Short title:

2 Natural variation in *B. distachyon* flowering time

3

4

5

6 Corresponding authors:

7 John H. Doonan

8 Institute of Biological, Environmental and Rural Sciences

9 Aberystwyth University

10 Aberystwyth

11 SY23 3DA

12 United Kingdom

13 Tel: +44 (0) 1970 823080

14 Email: john.doonan@aber.ac.uk

15

16 Matthew J. Moscou

17 The Sainsbury Laboratory

18 Norwich Research Park

19 Norwich

20 NR4 7UH

21 United Kingdom

22 Tel: +44 (0)1603 450296

23 Email: matthew.moscou@sainsbury-laboratory.ac.uk

24 **Title:**

25 Natural variation in *Brachypodium* links vernalization and flowering time loci as major
26 flowering determinants

27

28

29 **Authors:**

30 Jan Bettgenhaeuser¹, Fiona M.K. Corke^{2,3}, Magdalena Opanowicz³, Phon Green¹, Inmaculada
31 Hernández-Pinzón¹, John H. Doonan^{2,3}, Matthew J. Moscou^{1,4}

32

33 **Affiliations:**

34 ¹The Sainsbury Laboratory, Norwich, NR4 7UH, United Kingdom

35 ²Institute of Biological, Environmental and Rural Sciences, Aberystwyth University,
36 Aberystwyth, SY23 3DA, United Kingdom

37 ³John Innes Centre, Norwich, NR4 7UH, United Kingdom

38 ⁴School of Biological Sciences, University of East Anglia, Norwich, NR4 7TJ, United
39 Kingdom

40

41

42

43 **Onesentence summary:**

44 Standing genetic variation for flowering time in a non-domesticated grass encompasses
45 known and novel regulators.

46 **Footnotes:**

47

48 Author contributions

49 JB, FC, MO, JD, and MM conceived the study, and participated in its design and
50 coordination. PG and IHP participated in the experiments. JB, FC, JD, and MM wrote the
51 manuscript. All authors read and approved the final manuscript.

52

53

54 Funding information

55 The work was funded by the Biotechnology and Biological Sciences Research Council
56 Doctoral Training Programme (BB/F017294/1) and Institute Strategic Programme
57 (BB/J004553/1), the Gatsby Charitable Foundation, the Leverhulme Trust (Grant reference
58 10754), the 2Blades Foundation, and the Human Frontiers Science Program
59 (LT000218/2011).

60

61

62 Present addresses

63 Magdalena Opanowicz

64 Thermo Fisher Scientific, Paisley, PA4 9RF, United Kingdom

65

66

67 Corresponding authors email addresses

68 John H. Doonan – john.doonan@aber.ac.uk

69 Matthew J. Moscou – matthew.moscou@sainsbury-laboratory.ac.uk

70 **Abstract**

71 The domestication of plants is underscored by the selection of agriculturally favorable
72 developmental traits, including flowering time, which resulted in the creation of varieties
73 with altered growth habits. Research into the pathways underlying these growth habits in
74 cereals has highlighted the role of three main flowering regulators: *VRN1*, *VRN2*, and *FT*.
75 Previous reverse genetic studies suggested that the roles of *VRN1* and *FT* are conserved in
76 *Brachypodium distachyon*, yet identified considerable ambiguity surrounding the role of
77 *VRN2*. To investigate the natural diversity governing flowering time pathways in a non-
78 domesticated grass, the reference *B. distachyon* accession Bd21 was crossed with the
79 vernalization-dependent accession ABR6. Resequencing of ABR6 allowed the creation of a
80 SNP-based genetic map at the F₄ stage of the mapping population. Flowering time was
81 evaluated in F_{4:5} families in five environmental conditions and three major loci were found to
82 govern flowering time. Interestingly, two of these loci colocalize with the *B. distachyon*
83 homologs of the major flowering pathway genes *VRN2* and *FT*, whereas no linkage was
84 observed at *VRN1*. Characterization of these candidates identified sequence and expression
85 variation between the two parental genotypes, which may explain the contrasting growth
86 habits. However, the identification of additional QTLs suggests that greater complexity
87 underlies flowering time in this non-domesticated system. Studying the interaction of these
88 regulators in *B. distachyon* provides insights into the evolutionary context of flowering time
89 regulation in the Poaceae, as well as elucidates the way humans have utilized the natural
90 variation present in grasses to create modern temperate cereals.

91 **Introduction**

92 Coordination of flowering time with geographic location and seasonal weather patterns has a
93 profound effect on flowering and reproductive success (Amasino, 2010). The mechanisms
94 underpinning this coordination are of great interest for understanding plant behavior and
95 distribution within natural ecosystems (Wilczek et al., 2010). Plants that fail to flower at the
96 appropriate time are unlikely to be maximally fertile and therefore will be less competitive in
97 the longer term. Likewise, optimal flowering time in crops is important for yield and quality:
98 seed and fruit crops need to flower early enough to allow ripening or to utilize seasonal rains,
99 while delayed flowering may be advantageous for leaf and forage crops (Distelfeld et al.,
100 2009; Jung and Müller, 2009).

101

102 Although developmental progression towards flowering can be modulated in several ways,
103 many plants have evolved means to detect seasonal episodes of cold weather and adjust their
104 flowering time accordingly, a process known as vernalization (Ream et al., 2012). Despite the
105 importance of flowering time, the molecular and genetic mechanisms underlying this
106 dependency have been studied in only a few systems, notably the Brassicaceae, Poaceae, and
107 Amaranthaceae (Andrés and Coupland, 2012; Ream et al., 2012). Three major
108 *VERNALIZATION* (*VRN*) genes appear to act in a regulatory loop in temperate grasses. The
109 wheat *VRN1* gene is a MADS-box transcription factor, which is induced in the cold (Yan et
110 al., 2003; Andrés and Coupland, 2012). This gene is related to the *Arabidopsis thaliana* genes
111 *APETALA1* and *FRUITFUL* (Yan et al., 2003; Andrés and Coupland, 2012). *VRN2* encodes a
112 small CCT-domain protein (Yan et al., 2004) that is repressed by *VRN1* and in turn represses
113 *FLOWERING LOCUS T* (*FT*), a strong universal promoter of flowering (Kardailsky et al.,
114 1999; Yan et al., 2006; Andrés and Coupland, 2012; Ream et al., 2012). In cereals, active
115 *VRN2* alleles are necessary for a vernalization requirement. Spring barley and spring wheat
116 varieties, which do not require vernalization to flower, either lack *VRN2* (Dubcovsky et al.,
117 2005; Karsai et al., 2005; von Zitzewitz et al., 2005), have point mutations in the conserved
118 CCT domain (Yan et al., 2004), or possess dominant constitutively active alleles of *VRN1*
119 (repressor of *VRN2*) (Yan et al., 2003; Fu et al., 2005) or *FT* (repressed by *VRN2*) (Yan et al.,
120 2006).

121

122 Investigations on the regulation of flowering in the Poaceae have focused on rice (*Oryza*
123 *sativa*), wheat (*Triticum aestivum*), and barley (*Hordeum vulgare*), all domesticated species
124 that have been heavily subjected to human selection over the past 10,000 years. Little

125 information is available on wild species within this family that have not been subjected to
126 human selection. Such a study could provide additional insights into the standing variation
127 present within wild systems and its likely pre-domestication adaptive significance in the
128 Poaceae (Schwartz et al., 2010). A favorable species for such a study is *Brachypodium*
129 *distachyon*, a small, wild grass, with a sequenced and annotated genome. *B. distachyon* was
130 originally developed as a model system for the agronomically important temperate cereals
131 (Draper et al., 2001; Opanowicz et al., 2008; The International Brachypodium Initiative,
132 2010; Catalán et al., 2014). With the recent availability of geographically dispersed diversity
133 collections, we can ask how wild grasses have adapted to different climatic zones.

134

135 Previous studies have begun to explore the molecular basis of vernalization in this system.
136 Higgins et al. (2010) identified homologs of the various flowering pathway genes in *B.*
137 *distachyon*, and several mainly reverse genetic studies have focused on characterizing these
138 genes further (Schwartz et al., 2010; Lv et al., 2014; Ream et al., 2014; Woods et al., 2014;
139 Woods et al., 2016). Schwartz et al. (2010) did not find complete correlation between
140 expression of *VRN1* and flowering and hypothesized that *VRN1* could therefore have
141 different activity or roles that are dependent on the genetic background. Yet, Ream et al.
142 (2014) found low *VRN1* and *FT* levels in *B. distachyon* accessions with delayed flowering,
143 suggesting a conserved role of these homologs. Further support for a conserved role of *VRN1*
144 and *FT* comes from the observation that overexpression of these genes leads to extremely
145 early flowering (Lv et al., 2014; Ream et al., 2014) and RNAi-based silencing of *FT* and
146 amiRNA-based silencing of *VRN1* prevent flowering (Lv et al., 2014; Woods et al., 2016).
147 The role of *VRN2* in *B. distachyon* is less clear. Higgins et al. (2010) failed to identify a
148 homolog of *VRN2* in *B. distachyon*; however, other studies identified Bradi3g10010 as the
149 best candidate for the *B. distachyon* *VRN2* homolog (Schwartz et al., 2010; Ream et al.,
150 2012). Recent research supports the functional conservation of *VRN2* in the role as a
151 flowering repressor, but suggests that the regulatory interaction between *VRN1* and *VRN2*
152 evolved after the diversification of the Brachypodieae and the core Pooideae (e.g. wheat and
153 barley) (Woods et al., 2016).

154

155 To date most studies on the regulation of flowering time of *B. distachyon* have used reverse
156 genetic approaches to implicate the role of previously characterized genes from other species
157 (Higgins et al., 2010; Lv et al., 2014; Ream et al., 2014; Woods et al., 2016), while only few
158 studies have used the natural variation present among *B. distachyon* accessions to identify

159 flowering loci (Tyler et al., 2016; Wilson et al., 2016). Currently lacking is the
160 characterization of loci that control variation in flowering time in a biparental *B. distachyon*
161 mapping population. The Iraqi reference accession Bd21 does not require vernalization
162 (Vogel et al., 2006; Garvin et al., 2008) and in addition, vernalization does not greatly reduce
163 time to flowering in a 16 h or 20 h photoperiod (Schwartz et al., 2010; Ream et al., 2014). In
164 contrast, the Spanish accession ABR6 can be induced to flower following a six-week
165 vernalization period (Draper et al., 2001; Routledge et al., 2004).

166

167 In this paper, we report on the genetic architecture underlying flowering time in a mapping
168 population developed from ABR6 and Bd21. We observed the segregation of vernalization
169 dependency during population advancement (Figure 1) and characterized the genetic basis of
170 this dependency in detail at the F_{4.5} stage in multiple environments. The ability to flower
171 without vernalization was linked to three major loci, two of which colocalize with the *B.*
172 *distachyon* homologs of *VRN2* and *FT*. Notably, our results further support the role of the
173 *VRN2* locus as a conserved flowering time regulator in *B. distachyon*.

174

175

176

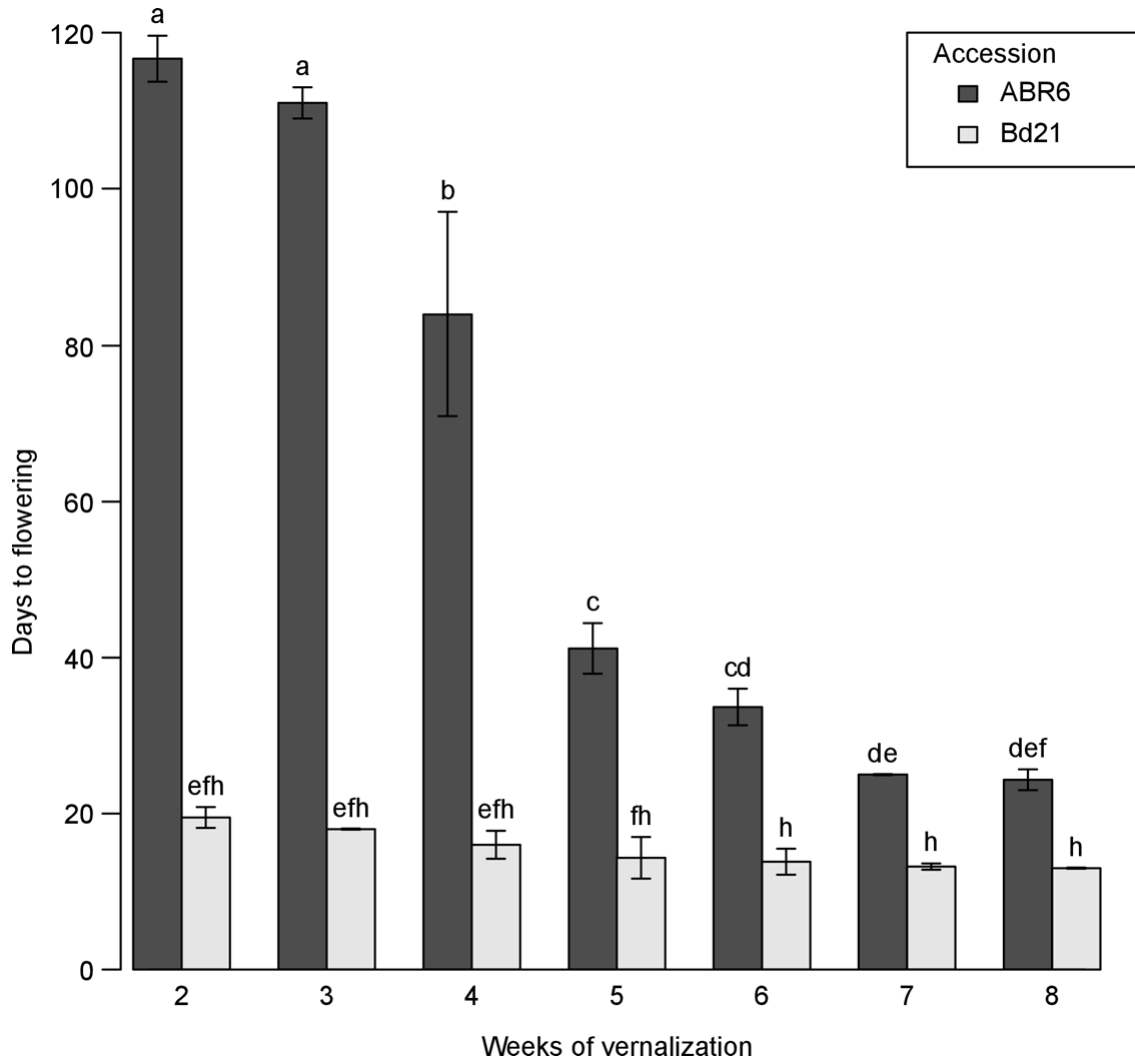


177 Results

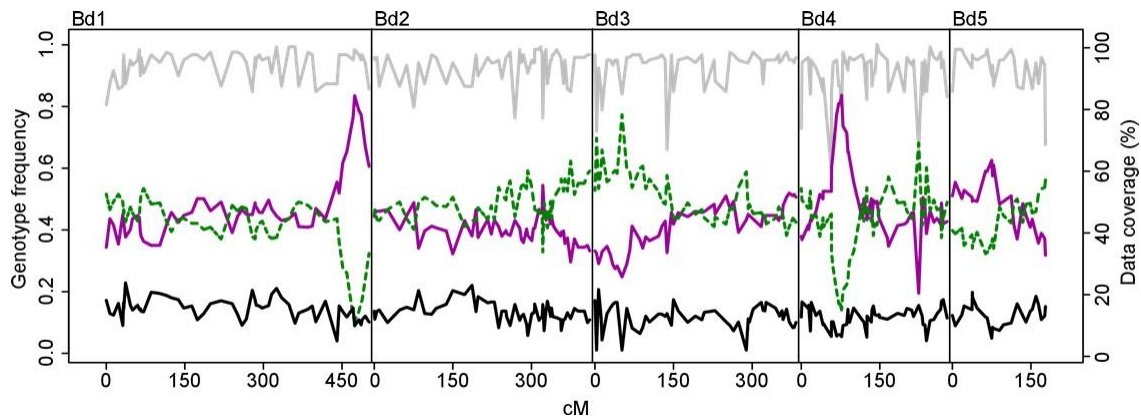
178

179 *Development of a B. distachyon mapping population between geographically and*
180 *phenotypically distinct accessions*

181 Initial investigations into the flowering time of ABR6 and Bd21 in response to different
182 vernalization periods showed contrasting effects on the two accessions (Figure 1 and Figure
183 2). ABR6 responded strongly to increasing vernalization times with a reduction in flowering
184 by 93 days, ranging from 117 days for a two-week vernalization period to 24 days for an
185 eight-week vernalization period. This reduction in flowering time for ABR6 was not linear
186 and the greatest drop of 43 days occurred between four and five weeks of vernalization
187 (Figure 2). In contrast, no statistically significant difference was found with respect to the
188 vernalization response of Bd21, although a consistent trend towards a reduced flowering time
189 was observed. A cross was generated from these phenotypically diverse accessions for the
190 creation of a recombinant inbred line population. To develop a SNP-based genetic map,
191 ABR6 was resequenced and reads were aligned to the reference genome. A total of 1.36
192 million putative SNPs were identified between ABR6 and Bd21, of which 711,052
193 constituted non-ambiguous polymorphisms based on a minimum coverage of 15x and a strict
194 threshold for SNP calling (i.e. 100% of reads with an ABR6 allele, 0% of reads with a Bd21

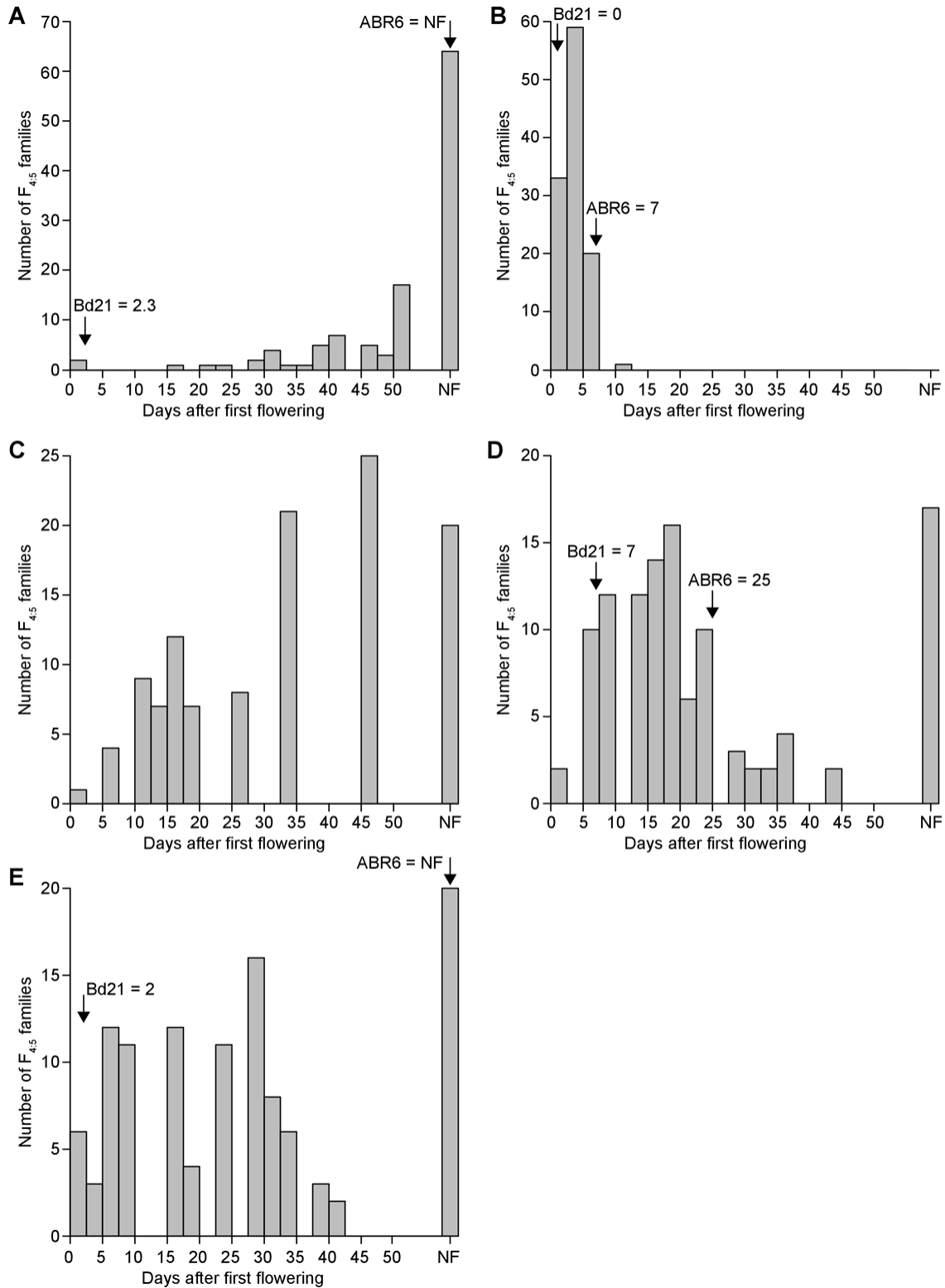


195 allele). Following iterative cycles of marker selection, the final genetic map consists of 252
 196 non-redundant markers and has a cumulative size of 1,753 cM (Supplemental Figure S1).
 197 This size is comparable to the previously characterized Bd3-1 x Bd21 mapping population
 198 (Huo et al., 2011) and confirms that *B. distachyon* has a high rate of recombination compared
 199 to other grass species. The quality of the genetic map was verified by assessing the two-way
 200 recombination fractions for all 252 markers (Supplemental Figure S2). All five chromosomes
 201 were scanned for segregation distortion by comparing observed and expected genotype
 202 frequencies for each marker. The expected heterozygosity at the F₄ stage is 12.50% and the
 203 expected parental allele frequencies are 43.75% for ABR6 and Bd21 alleles, respectively.
 204 Although all five chromosomes contained regions of potential segregation distortion (Figure
 205 3), only two loci on chromosomes Bd1 (peak at 474.1 cM) and Bd4 (peak at 77.0 cM)
 206 deviated significantly from these expected frequencies.
 207

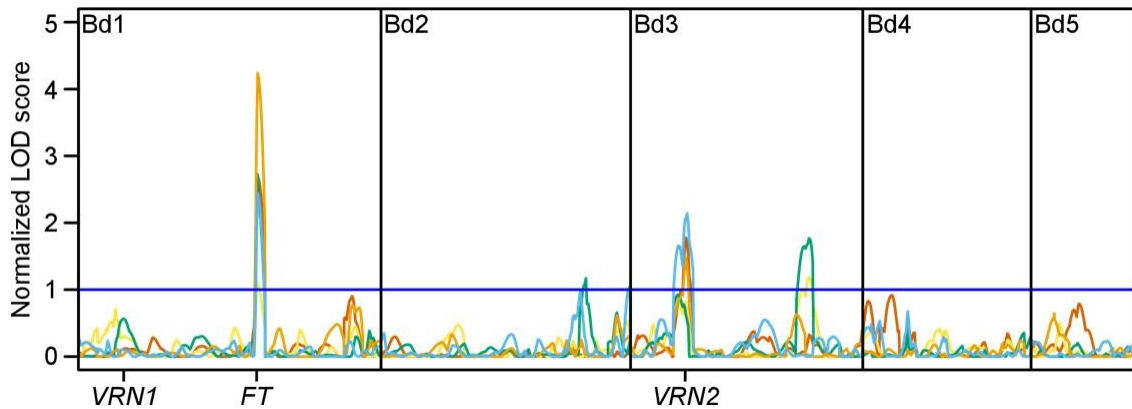


208 *Multiple QTLs control flowering in the ABR6 x Bd21 mapping population*

209 We evaluated the ABR6 x Bd21 F_{4:5} population in a number of environments to identify the
 210 genetic architecture underlying flowering time (Supplemental Table S1 and Supplemental
 211 Data S1). Four sets of the population were grown without vernalization, whereas in one
 212 additional set flowering was scored in response to six weeks of vernalization. In all
 213 experiments, the population was exposed to natural light, although in three experiments
 214 supplemental light was used to ensure a minimum 16 h or 20 h growth period. In addition,
 215 two experiments did not have any temperature control (i.e. plants were exposed to the natural
 216 temperature in the greenhouse), three experiments had the temperature controlled at
 217 22°C/20°C during light/dark cycles, and one experiment had the temperature maintained at a
 218 minimum of 18°C/11.5°C during light/dark cycles. Analysis of the non-vernalized
 219 environments revealed a bimodal distribution between families that flowered and families
 220 that did not flower (Figure 4). However, considerable residual variation in flowering time
 221 existed among the flowering families. For example, in Environment 5 flowering occurred
 222 over a 42-day period from 63 days to 105 days after germination (Figure 4E). Flowering in
 223 the other non-vernalized environments occurred over a similar time period (Figure 4).
 224 Interestingly, transgressive segregation for early and late flowering phenotypes was observed
 225 in Environment 4 (Figure 4D). Phenotypes in the vernalized environment were heavily
 226 skewed towards early flowering (Figure 4B). Only limited residual variation existed among
 227 the vernalized F_{4:5} families and all plants flowered within 11 days from the first observation
 228 of flowering in the population. The variation in flowering time for all five environments was
 229 found to be not normally distributed. Among these diverse environments, QTL analyses
 230 using binary and non-parametric models were conservative in detecting QTLs controlling
 231 flowering time (*qFLT*) (Supplemental Table S2 and Supplemental Table S3), whereas
 232 transformation of flowering time consistently identified QTLs between environments
 233 (Supplemental Table S4 and Supplemental Table S5; Table 1 and Table 2). Three major



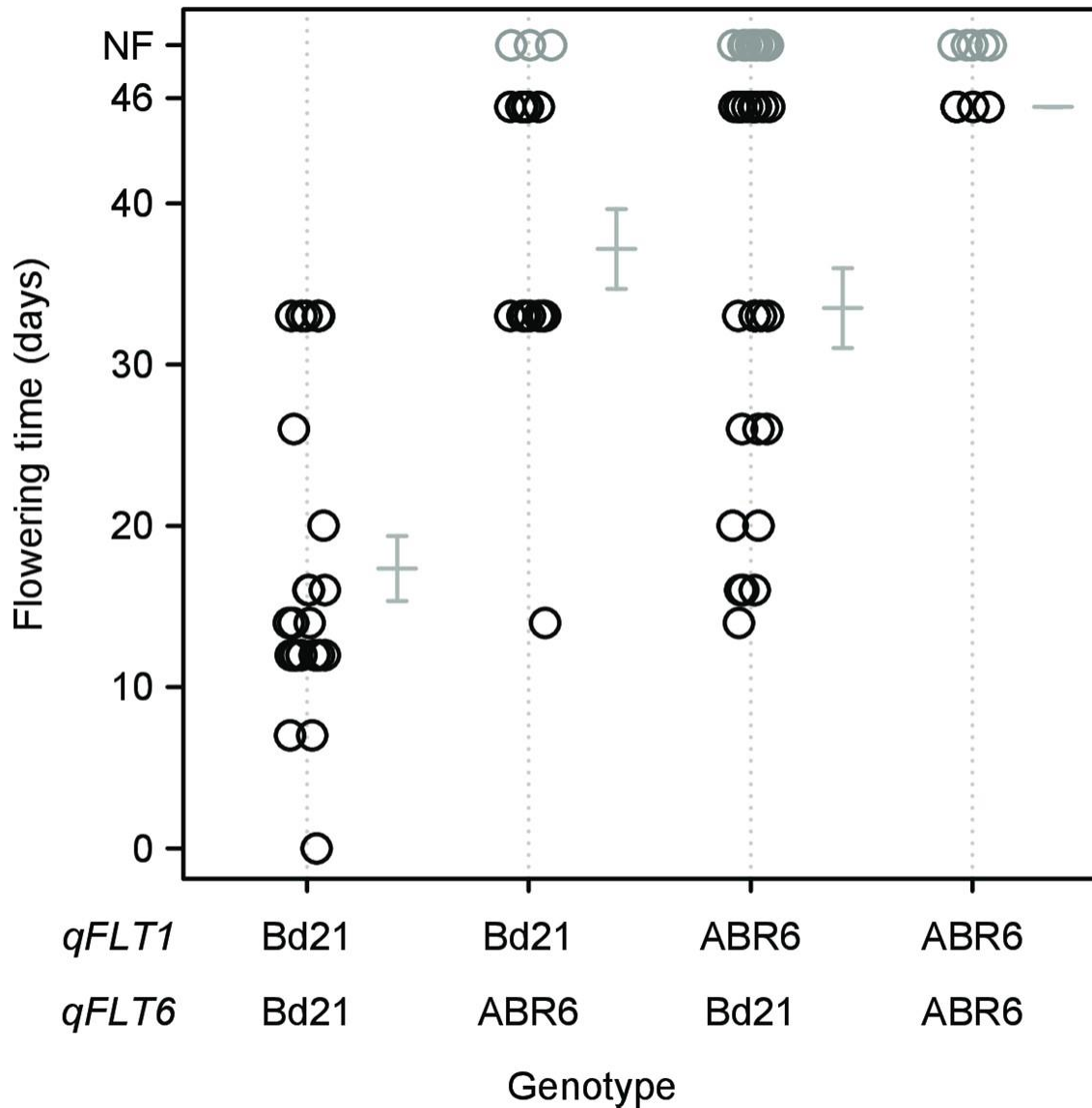
234 QTLs were identified on chromosomes Bd1 and Bd3 that were robustly observed using
 235 parametric and non-parametric mapping approaches (Table 1 and Table 2; Figure 5). The
 236 QTL on Bd1 (*qFLT1*, peak marker Bd1_47808182) appeared to be the major locus governing
 237 flowering time in this population, as it was the major QTL in all five environments,



238 explaining the most phenotypic variation (phenotypic variance explained; PVE) compared to
 239 any other QTL (Table 2). PVE values for this locus ranged from 15.9% to 37.5%. Another
 240 QTL on Bd3 (*qFLT6*, peak marker Bd3_8029207) was also detected in all five studies,
 241 though its contribution was only significant in three environments. PVE values for the
 242 statistically significant QTLs ranged from 11.8% to 18.7%. Bd21 alleles at these two loci
 243 promoted early flowering, whereas individuals with ABR6 alleles at both loci had maximal
 244 flowering time or did not flower within the timescale of the experiment (Figure 6).
 245 Interestingly, in the two environments where this former locus did not have a significant
 246 contribution, two other QTLs were identified. A QTL on Bd3 (*qFLT7*, peak marker
 247 Bd3_44806296) explained 13.6% and 14.0% of the variation observed in these studies and a
 248 QTL on Bd2 (*qFLT3*, peak marker Bd2_53097824) was identified through a combination of
 249 non-parametric and parametric analyses of Environments 4 and 5. Additional QTLs on Bd1
 250 (*qFLT2*), Bd2 (*qFLT4*), Bd3 (*qFLT5*), and Bd4 (*qFLT8*) were not significant in more than
 251 one of the environments tested (Table 1).

252

253 Previous studies identified the *B. distachyon* homologs of flowering regulators from
 254 *Arabidopsis*, wheat, barley, and rice (Higgins et al., 2010; Ream et al., 2014). The one-LOD
 255 support intervals of all statistically significant QTLs were combined to identify the maximal
 256 one-LOD support interval for each QTL. Several of the previously identified *B. distachyon*
 257 homologs of flowering regulators are candidate genes underlying these QTLs (Table 3).
 258 Although several homologs fall within the one-LOD support intervals of *qFLT1* on Bd1
 259 (292.1 - 305.6 cM) and *qFLT6* on the short arm of Bd3 (72.9 - 97.0 cM), these loci also
 260 harbor the *B. distachyon* homologs of *FT* (Bradi1g48830) and *VRN2* (Bradi3g10010), which
 261 have been previously implicated in flowering time regulation in *B. distachyon* through a
 262 series of mainly reverse genetic studies (Lv et al., 2014; Ream et al., 2014; Woods et al.,
 263 2014; Woods et al., 2016).

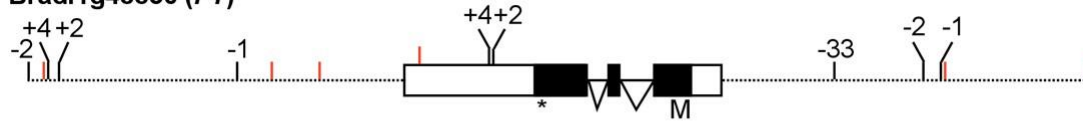
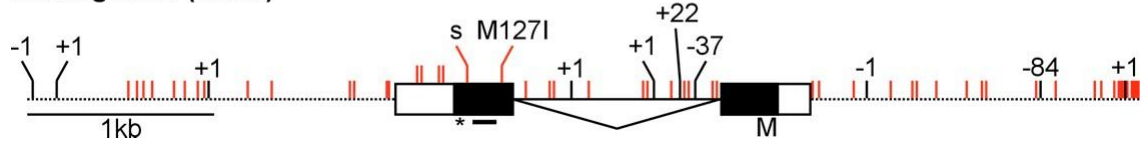


264

265 *Natural variation in FT and VRN2*

266 Analysis of the resequencing and RNAseq data allowed an initial evaluation of candidate
 267 genes underlying these QTLs. A *de novo* assembly was created from the ABR6 resequencing
 268 reads and the resulting contigs were probed with the Bd21 sequences of *FT* (Bradi1g48830)
 269 and *VRN2* (Bradi3g10010), enabling the identification of structural variation between ABR6
 270 and Bd21 (Figure 7; Supplemental Table S6). Spliced alignment of RNAseq reads permits
 271 further characterization of candidate genes underlying an identified QTL through the
 272 confirmation of polymorphisms between two parental genotypes, verification of annotated
 273 candidate gene models, qualitative assessment of expression of candidate genes in the
 274 sampled tissue, and discovery of potential splice variants.

275

Bradi1g48830 (FT)**Bradi3g10010 (VRN2)**

276 No polymorphisms were found in the coding sequence of Bradi1g48830, the *B. distachyon*
 277 homolog of *FT*. However, two indels (two and four bp, respectively) and a SNP mapped to
 278 the 3'-UTR. Additionally, two SNPs and three indels (including a 33 bp indel 590 bps
 279 upstream of Bradi1g48830) were found in the promoter region (2 kb upstream). The
 280 terminator region (2 kb downstream) contained three SNPs and four indels. Bradi1g48830
 281 was not expressed in ABR6 and barely detectable in Bd21 (only two reads mapped to the
 282 gene). Owing to the low expression, it was not possible to confirm the published gene model
 283 with our RNAseq data.

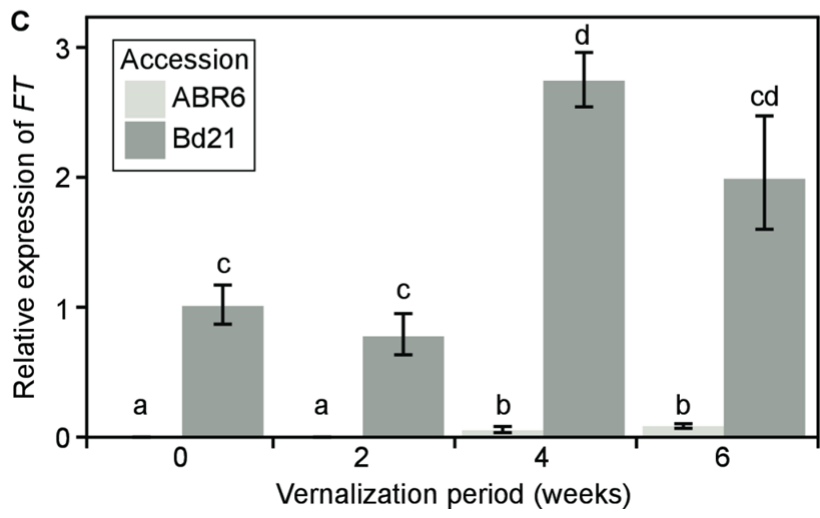
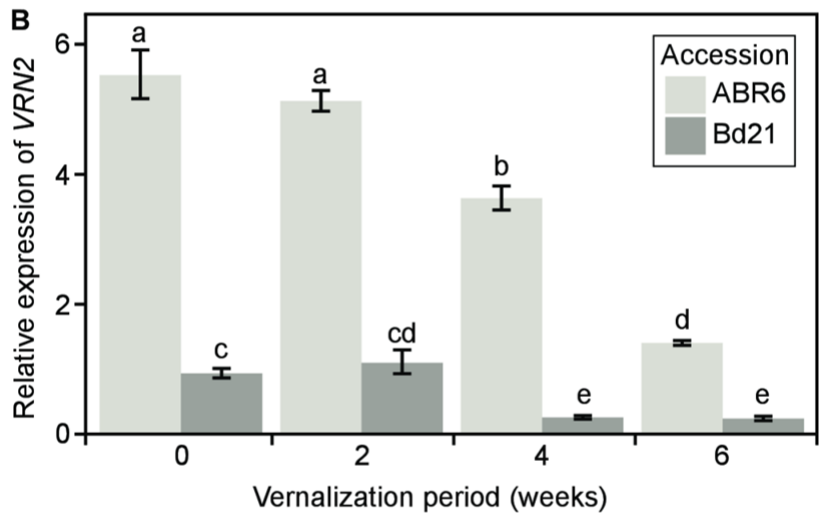
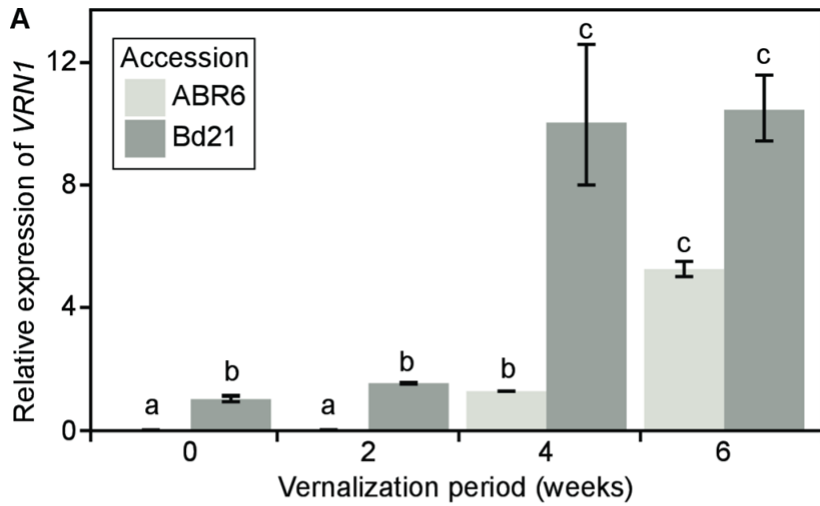
284

285 Greater sequence variation was observed at Bradi3g10010, the *B. distachyon* homolog of
 286 *VRN2*, and its flanking regions. Only 1.9 kb of the promoter region is present on the
 287 Bradi3g10010 contig, but this region contains 29 SNPs and three indels (including an 84 bp
 288 indel 1.4 kb upstream of Bradi3g10010). The 2 kb terminator region contains 14 SNPs and
 289 three 1 bp indels. Additionally, 11 SNPs and four indels (including a 37 bp and a 22 bp indel)
 290 were localized in the intron, two SNPs in the coding sequence, and four SNPs in the 3'-UTR.
 291 Bradi3g10010 was expressed in leaves from both Bd21 and ABR6 and spliced alignment of
 292 RNAseq reads confirmed the published annotation of Bradi3g10010 for both ABR6 and
 293 Bd21. Moreover, the six SNPs predicted in the exons were supported by the RNAseq data
 294 and these may contribute to the observed effect on flowering time in this mapping population.
 295 Two SNPs map to the annotated coding sequence and four SNPs map to the 3'-UTR. One of
 296 the two SNPs in the annotated coding sequence is predicted to cause a non-synonymous
 297 mutation (Figure 7).

298

299 *Expression of VRN1, VRN2, and FT in response to vernalization*

300 To understand the transcriptional dynamics of *VRN1*, *VRN2*, and *FT* in response to
 301 vernalization, we assessed steady state levels of mRNA expression in plants at the fourth leaf
 302 stage after exposure to two, four, and six weeks of vernalization at 5°C or to no vernalization



303 (Figure 8). *VRN1* and *FT* had a similar pattern in steady state levels of gene expression in
 304 response to vernalization (Figure 8A and 8C). For both genes, very low levels of expression
 305 were observed in ABR6, whereas Bd21 had fairly high levels of transcript abundance. After
 306 experiencing four weeks of vernalization, ABR6 had similar levels of *VRN1* transcript as

307 Bd21 without vernalization treatment. In contrast, *FT* expression had a marginal increase
308 after four and six weeks of vernalization in ABR6 relative to no vernalization or two weeks
309 of vernalization. *FT* expression levels were significantly lower than Bd21 across all periods
310 of vernalization. Both *VRN1* and *FT* expression increased significantly between Bd21
311 examples vernalized for two or four weeks. *VRN2* expression in ABR6 was inversely
312 correlated with the length of vernalization, with similar levels of expression after no
313 vernalization and two weeks vernalization and increasingly lower levels of expression after
314 four and six weeks of vernalization (Figure 8B). Bd21 exhibited a similar reduction in *VRN2*
315 expression, although lower levels of expression were observed without vernalization
316 compared to ABR6 with six weeks vernalization. The trends of all three genes highlighted the
317 importance of four weeks of vernalization as the inflection point in transcriptional abundance,
318 which coincides with a significant reduction in days to flowering in ABR6 (Figure 2).
319
320
321

322 Discussion

323

324 In our advancement of the ABR6 x Bd21 RIL population, we observed substantial variation
325 in flowering time. To define the genetic architecture of flowering time, we developed a
326 comprehensive genetic map and assessed F_{4:5} families in multiple environments. We
327 uncovered three major QTLs, with two QTLs coincident with the *B. distachyon* homologs of
328 *VRN2* and *FT*. Interestingly, *VRN1* was not associated with flowering time and was found to
329 have no mutations within the transcribed sequence (Supplemental Table S6). Further minor
330 effect QTLs were identified, suggesting that additional regulators play a role in controlling
331 flowering time in *B. distachyon*.

332

333 *Segregation distortion in the ABR6 x Bd21 population*

334 Segregation distortion is a common observation in the development of mapping populations
335 in plants, including grasses such as rice, *Aegilops*, maize, or barley (Xu et al., 1997; Faris et
336 al., 1998; Lu et al., 2002; Muñoz-Amatriaín et al., 2011). In the ABR6 x Bd21 population,
337 significant deviation from expected genotype frequencies was observed at two loci on
338 chromosomes Bd1 and Bd4 (Figure 3). Interestingly, heterozygosity was not affected at these
339 loci, but the ABR6 allele was overrepresented. It is likely that these loci are linked to traits
340 that were inadvertently selected during population advancement based on genetic and/or
341 environmental factors. Several genetic mechanisms can contribute to segregation distortion in
342 intraspecific crosses, including hybrid necrosis (Bomblies and Weigel, 2007), genes involved
343 in vernalization requirement and flowering time (such as the *vrn2* locus in the Haruna Nijo x
344 OHU602 doubled-haploid barley population (Muñoz-Amatriaín et al., 2011)), or preferential
345 transmission of a specific parental genotype. While segregation distortion at these loci was
346 not associated with the identified flowering time QTLs, canonical resistance genes encoding
347 nucleotide-binding, leucine-rich repeat proteins are present at the Bd4 locus (Bomblies et al.,
348 2007; Tan and Wu, 2012).

349

350 *The genetic architecture of flowering time in B. distachyon*

351 In *Arabidopsis*, natural variation has been used as a complementary forward genetics-based
352 approach for investigating flowering time (Koornneef et al., 2004). In our work, we identified
353 two major QTLs controlling flowering time (*qFLT1* and *qFLT6*; Figure 6) in both vernalized
354 and non-vernalized environments that colocalized with the *B. distachyon* homologs of *FT*
355 (Bradi1g48830) and *VRN2* (Bradi3g10010). These observations are consistent with previous

356 reverse genetic studies on the role of *FT* and *VRN2* in controlling flowering time (Lv et al.,
357 2014; Ream et al., 2014; Woods et al., 2014; Woods et al., 2016). Two additional QTLs on
358 chromosomes Bd2 (*qFLT3*) and Bd3 (*qFLT7*) were detected in two environments, whereas
359 three minor effect QTLs (*qFLT2*, *qFLT4*, *qFLT5*, and *qFLT8*) were found in individual
360 environments only. Two recent genome-wide association studies (GWAS) used the natural
361 variation found within *B. distachyon* germplasm to identify SNPs associated with flowering
362 time (Tyler et al., 2016; Wilson et al., 2016). Tyler *et al.* (2016) identified nine significant
363 marker-trait associations, none of which overlap with the QTLs identified in our study. In
364 contrast, Wilson *et al.* (2016) identified a much simpler genetic architecture consisting of
365 three significant marker-trait associations, one of which could be linked to *FT*. These
366 additional QTLs and marker-trait associations identified in our study and the GWAS studies
367 could either correspond to one of the identified homologs of flowering genes in *B. distachyon*
368 (Table 3; compare Higgins *et al.* 2010) or constitute novel loci as hypothesized by Schwartz
369 *et al.* (2010). With the exception of the proximal QTL on Bd2 (*qFLT3*), all QTLs in our study
370 were contributed by ABR6 (Table 1). Bd21 has previously been classified as a “spring
371 annual” (Schwartz et al., 2010) or “extremely rapid flowering” (Ream et al., 2014). However,
372 increased vernalization times still led to a modest reduction in flowering time (Figure 2),
373 which is explained by the detection of a QTL contributed by Bd21.

374

375 We hypothesized that structural variation between ABR6 and Bd21 would underlie the
376 observed variation in flowering time. No structural variation in *FT* was observed between
377 ABR6 and Bd21 in the coding sequence, however, several indels map to the promoter region
378 (Figure 7). These polymorphisms may explain expression differences between these two
379 accessions. As expected, no *FT* expression was found in ABR6 seedlings, and only two Bd21
380 RNAseq reads mapped to this gene. Steady-state expression levels of *FT* in the fourth leaf
381 were significantly lower in ABR6 relative to Bd21 without vernalization (Figure 8C). After
382 four weeks vernalization, *FT* expression levels increased in ABR6, although they were
383 significantly lower than Bd21 steady-state levels after any level of vernalization. It was
384 previously shown that in barley, wheat, and *B. distachyon*, *FT* expression is upregulated after
385 vernalization (Sasani et al., 2009; Chen and Dubcovsky, 2012; Ream et al., 2014). Our
386 observations indicate that *FT* is expressed in Bd21 and increases less than *VRN1* in response
387 to vernalization. In contrast, *FT* in ABR6 only increases marginally after four weeks of
388 vernalization and remains significantly below the levels observed in Bd21 after no
389 vernalization.

390

391 Interestingly, an intact copy of the flowering repressor *VRN2* is also present in Bd21 (Ream
392 et al., 2012), which does not have a strong vernalization response (Vogel et al., 2006; Garvin
393 et al., 2008). The lack of vernalization requirement in some *B. distachyon* accessions cannot,
394 therefore, be explained by an absence of *VRN2* (Ream et al., 2014). Intriguingly, early-
395 flowering mutants identified in genetic screens have thus far not mapped in the *VRN2* region
396 (Ream et al., 2014). Moreover, expression levels for *VRN2* also did not vary among early and
397 late flowering accessions and *VRN2* mRNA levels are likely not rate limiting (Ream et al.,
398 2014). An earlier study by Schwartz *et al.* (2010) described potential correlation between
399 different *VRN2* alleles and flowering time. The authors did not rule out the effects of
400 population structure and proposed that elucidating the role of *VRN2* in *B. distachyon* will
401 require more in-depth genetic studies. A recent comprehensive analysis of population
402 structure in *B. distachyon* collections revealed that flowering time, and not geographic origin,
403 is indeed the major distinguishing factor between genotypically distinct clusters (Tyler et al.,
404 2016). Our results confirm *VRN2* as an important flowering regulator in the ABR6 x Bd21
405 mapping population and highlight structural and expression variation between parental
406 accessions. However, none of the SNPs identified in the coding sequence map to the CCT
407 domain. A point mutation in this domain results in a spring growth habit in cultivated
408 *Triticum monococcum* accessions (Yan et al., 2004). It is unclear whether the structural
409 variation surrounding *VRN2* corresponds to the allelic variation observed by Schwartz *et al.*
410 (2010). Woods and Amasino (2016) hypothesize that even though *VRN2* may not be involved
411 in vernalization control in *B. distachyon*, it may still possess an ancestral role in flowering
412 regulation. This is further supported by the observation that *VRN2* expression is not
413 controlled by *VRN1* in *B. distachyon*, yet *VRN2* was found to be a functional repressor of
414 flowering in this species (Woods et al., 2016). We observed a negative correlation between
415 *VRN2* transcript accumulation and vernalization period in ABR6 and Bd21 (Figure 8B).
416 Similar decreases were observed for ABR6 and Bd21, although transcript abundance in Bd21
417 were significantly lower than ABR6 under any vernalization period. Therefore, our
418 identification of natural variation in *VRN2* among geographically diverse *B. distachyon*
419 accessions further supports *VRN2* as a core flowering regulator in this non-domesticated
420 grass.

421

422 In our study of the natural variation between two morphologically and geographically diverse
423 *B. distachyon* accessions we failed to implicate *VRN1* as a flowering regulator. However,

424 *VRN1* expression during and after cold treatment and the failure of *VRN1* silenced lines to
425 flower suggests a conserved role of *VRN1* as a promoter of flowering (Woods and Amasino,
426 2016; Woods et al., 2016). Interestingly, a QTL in the Bd21 x Bd1-1 *B. distachyon* mapping
427 population colocalized with *VRN1* and the light receptor *PHYTOCHROME C (PHYC)*
428 (Woods et al., 2016). Between ABR6 and Bd21, sequence variation was found in the
429 promoter and terminator regions of *VRN1* and a strong positive correlation was observed with
430 extended periods of vernalization (Figure 8A), particularly at four weeks vernalization, which
431 was a critical inflection point for flowering time in ABR6. Despite this sequence and
432 expression variation, *VRN1* was not found to contribute to flowering time in the ABR6 x
433 Bd21 mapping population. Interestingly, an assessment of allelic variation in 53 *B.*
434 *distachyon* accessions currently available in Phytozome (Version 11.0.2,
435 <https://phytozome.jgi.doe.gov>) found that none of these accessions possess structural
436 variation in the *VRN1* annotated coding sequence. These findings suggest that *VRN1* is a
437 crucial regulator of flowering in *B. distachyon* and under strong selection pressure.

438

439

440 **Conclusions**

441

442 Thanks to their economic and evolutionary importance, flowering time pathways are of
443 particular interest in the cereals and related grasses. Our report adds to this body of research
444 by using natural variation to map vernalization dependency in a *B. distachyon* mapping
445 population. Since *B. distachyon* is partly sympatric with the wild relatives of wheat and
446 barley, it seems likely that the species would have been subject to similar selective pressure
447 and therefore is a useful model for understanding pre-domestication or standing variation. We
448 investigated this standing variation by assessing segregation of flowering regulators in a
449 mapping population derived from two geographically diverse accessions of *B. distachyon*.
450 Notably, we found additional support for the roles of *FT* and *VRN2* in controlling flowering
451 in wild temperate grasses. Additionally, allelic variation may explain the ambiguity around
452 the role of the *VRN2* homolog observed in *B. distachyon*. Further fine-mapping will be
453 required to confirm the roles of these genes in *B. distachyon* flowering time. However, we
454 also detected novel components in the form of additional QTLs, which reflects the power of
455 studying natural variation in mapping populations derived from phenotypically diverse
456 parents. During population advancement, we have observed a variety of additional
457 morphological and pathological characteristics segregating in this population and it will serve

458 as a useful resource for other researchers investigating standing variation in non-domesticated
459 grasses.

460

461

462 **Materials and Methods**

463

464 *Plant growth for assessing ABR6 and Bd21 vernalization response*

465 Six seeds for ABR6 and Bd21 were germinated on paper (in darkness at room temperature)
466 and transferred to an equal mixture of the John Innes Cereal Mix and a peat and sand mix
467 (Vain et al., 2008) four days after germination. Vernalization was initiated 14 days after
468 germination for either two, three, four, five, six, seven, or eight weeks (8 h day length; 1.2
469 klux light intensity; 5°C). The different sets were staggered to ensure that all sets left
470 vernalization on the same date. After vernalization plants were grown in a Sanyo Versatile
471 Environmental Test Chamber (Model MLR-351; 16 h photoperiod; 8.0 klux light intensity;
472 22°C/20°C day/night temperatures) for 35 days and then transferred to a greenhouse without
473 light and temperature control (late April to mid July 2013; Norwich, UK). Days to flowering
474 was measured from the end of vernalization until the emergence of the first spike and was
475 averaged across all six biological replicates (only five replicates were available for Bd21 after
476 7 weeks of vernalization). Statistical significances were assessed by pairwise comparisons
477 using *t*-tests with pooled standard deviations and Bonferroni correction for multiple
478 comparisons.

479

480 *Resequencing of ABR6*

481 Seedlings were grown in a Sanyo Versatile Environmental Test Chamber (16h photoperiod;
482 8.0 klux light intensity; 22°C) in an equal mixture of the John Innes Cereal Mix and a peat
483 and sand mix. Seven-week-old plants were placed in darkness for three days prior to
484 collecting tissue. Genomic DNA was extracted using a standard CTAB protocol and a library
485 of 800 bp inserts was constructed and sequenced with 100 bp paired-end reads and an
486 estimated coverage of 25.8x on an Illumina HiSeq 2500. Library preparation and sequencing
487 was performed at The Genome Analysis Centre (Norwich, UK). The resulting reads were
488 mapped to the Bd21 reference sequence (Version 1)
489 (The International Brachypodium Initiative, 2010) with the Galaxy wrapper, which used the
490 BWA (Version 0.5.9) *aln* and *sampe* options (Li and Durbin, 2009). Polymorphisms between
491 ABR6 and Bd21 were identified with the *mpileup2snp* and *mpileup2indel* tools of *VarScan*

492 (Version 2.3.6) using default settings (Koboldt et al., 2009). A *de novo* assembly was created
493 from the raw ABR6 reads using default settings of the CLC Assembly Cell (Version 4.2.0)
494 and default parameters. Potential structural variation between ABR6 and Bd21 was
495 investigated by performing a BLAST search with the Bd21 regions of interest against the
496 ABR6 *de novo* assembly and mapping contigs for hits with at least 95% identity and an E-
497 value under $1e^{-20}$ to the Bd21 reference sequence (Version 3).

498

499 *Development of the ABR6 x Bd21 F₄ population and genetic map*

500 The *B. distachyon* accessions ABR6 and Bd21 were crossed and three ABR6 x Bd21 F₁
501 individuals, confirmed as hybrid by SSR marker analysis (data not shown), were allowed to
502 self-pollinate to generate a founder F₂ population comprised of 155 individuals. After single
503 seed descent, DNA was extracted from leaf tissue of 114 independent F₄ lines using a CTAB
504 gDNA extraction protocol modified for plate-based extraction (Dawson et al., 2016). SNPs
505 for genetic map construction were selected based on a previously characterized Bd21 x Bd3-1
506 F₂ genetic map to ensure an even distribution of markers relative to physical and genetic
507 distances (Huo et al., 2011). SNPs without additional sequence variation in a 120 bp window
508 were selected every 10 cM. The Agena Bioscience MassARRAY design suite was used to
509 develop 17 assays that genotyped 449 putative SNPs using the iPLEX Gold assay at the Iowa
510 State University Genomic Technologies Facility (Supplemental Data S2). Markers were
511 excluded for being monomorphic (106), dominant (34), or for missing data for the parental
512 controls (33). Heterozygous genotype calls for some markers were difficult to distinguish and
513 classified as missing data. Additional SNPs between ABR6 and Bd21 in six markers
514 developed for the Bd21 x Bd3-1 F₂ genetic map (Barbieri et al., 2012) were converted into
515 CAPS markers (Konieczny and Ausubel, 1993) (Supplemental Table S7). The integrity of
516 these 282 markers was evaluated using R/qtl (Version 1.33-7) recombination fraction plots
517 (Broman et al., 2003). Two markers were removed for not showing linkage and one marker
518 was moved to its correct position based on linkage. Genetic distances were calculated using
519 the Kosambi function in MapManager QTX (Version b20) (Manly et al., 2014). Removal of
520 unlinked and redundant markers produced a final ABR6 x Bd21 F₄ genetic map consisting of
521 252 SNP-based markers (Supplemental Data S3). Segregation distortion was assessed using a
522 chi-square test with Bonferroni correction for multiple comparisons.

523

524 *Plant growth and phenotyping of flowering time in the ABR6 x Bd21 F_{4:5} families*

525 Three to five plants for each of the 114 ABR6 x Bd21 F_{4:5} families were grown under five
526 different environmental conditions as detailed in Supplemental Table S1. For the
527 phenotyping performed in Aberystwyth, individual seeds were sown in 6 cm pots with a
528 mixture of 20% grit sand and 80% Levington F2 peat-based compost. Seeds were grown for
529 2 weeks in greenhouse conditions (22°C/20°C, natural light supplemented with 20 h lighting)
530 and then either maintained in the greenhouse or transferred to a vernalization room for six
531 weeks (16 h day length, 5°C). Plants were returned to the greenhouse following vernalization
532 and grown to maturity. Flowering time was defined as the emergence of the first
533 inflorescence and was measured from the first day that flowering was observed in the entire
534 mapping population. Flowering time was averaged across the individuals of an F_{4:5} family.
535 For the phenotyping performed in Norwich, plants were first subjected to growth conditions
536 and pathogen assays as described in Dawson *et al.* 2015. Plants were germinated in a peat-
537 based compost in 1 L pots and grown for six weeks in a controlled environment room
538 (18°C/11°C, 16 h light period). Six weeks post germination, the fourth or fifth leaf of each
539 plant was cut off for pathological assays. The plants were transplanted into 9 cm pots with an
540 equal mixture of the John Innes Cereal Mix and a peat and sand mix (Vain *et al.*, 2008) and
541 transferred to the respective growth environments for flowering assessment (Supplemental
542 Table S1). Flowering time was defined as the emergence of the first inflorescence within an
543 F_{4:5} family and was measured from the first day that flowering was observed in the entire
544 mapping population. Families that did not flower 60 days after emergence of the first
545 inflorescence in the mapping population were scored as not flowering.

546

547 *Quantitative trait locus analysis for flowering time*

548 Flowering phenotypes were assessed for normality using the Shapiro-Wilk test (Royston,
549 1982). In an initial analysis, phenotypic values were converted into a binary classification
550 based on whether families flowered (F) or did not flower (NF). Interval mapping was
551 performed with the *scanone* function in R/qtl under a *binary* model with conditional genotype
552 probabilities computed with default parameters and the Kosambi map function (Xu and
553 Atchley, 1996; Broman *et al.*, 2006). Simulation of genotypes was performed with a fixed
554 step distance of 2 cM, 128 simulation replicates, and a genotyping error rate of 0.001.
555 Statistical significance for QTLs was determined by performing 1,000 permutations and
556 controlled at $\alpha = 0.05$ (Doerge and Churchill, 1996). Non-parametric interval mapping was
557 performed with similar parameters in R/qtl under an *np* model (Kruglyak and Lander, 1995).

558 For parametric mapping, flowering time data was transformed (T) using the following
559 approaches: (T1) the removal of all F_{4:5} families that did not flower within the timescale of
560 the experiment, (T2) transforming all non-flowering phenotypic scores to one day above the
561 maximum observed, and (T3) transforming by ranking families according to their flowering
562 time. For the third transformation approach (T3), the earliest flowering family was given a
563 rank score of 1 and subsequent ordered families given incremental scores based on rank (2, 3,
564 4, etc.). When two or more families had shared flowering time, they were given the same
565 rank and the next ranked family was given an incremental rank score based on the number of
566 preceding shared rank families. Non-flowering families were given the next incremental rank
567 after the last flowering rank. For all three transformations, composite interval mapping was
568 performed under an additive model (H₀:H₁) using QTL Cartographer (Version 1.17j) with the
569 selection of five background markers, a walking speed of 2 cM, and a window size of 10 cM
570 (Zeng, 1993, 1994; Basten et al., 2004). Statistical significance for QTLs was determined by
571 performing 1,000 permutations with reselection of background markers and controlled at $\alpha =$
572 0.05 (Doerge and Churchill, 1996; Lauter et al., 2008). One-LOD support intervals were
573 estimated based on interval mapping (Lander and Botstein, 1989).

574

575 *RNAseq of ABR6 and Bd21*

576 Plants were grown in a controlled environment room with 16 h light at 22°C and fourth and
577 fifth leaves were harvested as soon as the fifth leaf was fully expanded (roughly 28 days after
578 germination). RNA was extracted using the TRI Reagent (Sigma-Aldrich®) according to the
579 manufacturer's specifications. TruSeq libraries were generated from total RNA and mean
580 insert sizes were 251 bp and 254 bp for ABR6 and Bd21, respectively. Library preparation
581 and sequencing was performed at The Genome Analysis Centre (Norwich, UK). Sequencing
582 was carried out using 150 bp paired-end reads on an Illumina HiSeq 2500 and ABR6 and
583 Bd21 yielded 38,867,987 and 37,566,711 raw reads, respectively. RNAseq data quality was
584 assessed with FastQC and reads were removed using Trimmomatic (Version 0.32) (Bolger et
585 al., 2014) with parameters set at ILLUMINACLIP:TruSeq 3-PE.fa:2:30:10, LEADING:3,
586 TRAILING:3, SLIDINGWINDOW:4:15, and MINLEN:100. These parameters will remove
587 all reads with adapter sequence, ambiguous bases, or a substantial reduction in read quality.
588 The sequenced reads were mapped to the Bd21 reference genome using the TopHat (Version
589 2.0.9) spliced alignment pipeline (Trapnell et al., 2009).

590

591 *RT-qPCR analyses*

592 ABR6 and Bd21 seeds were surface sterilized (70% ethanol for 30 seconds, washed in
593 autoclaved dH₂O, 1.3% sodium hypochlorite for 4 minutes, washed in autoclaved H₂O three
594 times), transferred to moistened Whatman filter paper, left at room temperature in darkness
595 overnight, and vernalized for either two, four, or six weeks (in darkness at 5°C). A control set
596 was surface sterilized and transferred to filter paper overnight, but not vernalized. Following
597 vernalization, plants were transferred to soil and grown in a Sanyo Versatile Environmental
598 Test Chamber in conditions similar to Environment 2 (20h photoperiod; 4.0 klux light
599 intensity; 22°C/20°C). Once fully expanded, fourth leaves were collected in the middle of the
600 photoperiod and flash frozen in liquid nitrogen.

601

602 Total RNA was extracted using TRI reagent according to manufacturer's instructions (Sigma-
603 Aldrich®). RNA samples were treated with DNase I (Roche) prior to cDNA synthesis.
604 Quality and quantity of RNA samples were assessed using a NanoDrop spectrophotometer
605 followed by agarose electrophoresis. First-strand cDNA was synthesized according to
606 manufacturer's instructions (Invitrogen). Briefly, 1 µg of total RNA, 1 µL of 0.5 µM poly-T
607 primers, and 1 µL of 10 mM dNTP were incubated at 65°C for 5 min and 4°C for 2 min, with
608 subsequent reverse transcription reactions performed using 2 µL of 10x reverse transcription
609 buffer, 4 µL of 25 mM MgCl₂, 2 µL of 0.1 M DTT, 1 µL of RNaseOUT (40 U/µL), and 1 µL
610 of SuperScript III reverse transcriptase (200 U/µL) at 50°C for 50 min. Reverse transcription
611 was inactivated by incubating at 85°C for 5 min and residual RNA was removed with the
612 addition of 1 µL Rnase H (2 U/µL) and incubation at 37°C for 20 min.

613

614 Quantitative real time PCR was performed in 20 µL reaction volumes using 10 µL of SYBR-
615 Green mix (Sigma-Aldrich), 1 µL of 10 µM forward and reverse primers, 4 µL water, and 4
616 µL of cDNA diluted 10-fold. The program for PCR amplification involved an initial
617 denaturation at 95°C for 3 min and then 40 cycles of 94°C for 10 sec, 60°C for 15 sec, and
618 72°C for 15 sec. Fluorescence data was collected at 72°C at the extension step and during the
619 melting curve program on a CFX96 Real-Time system (Bio-Rad).

620

621 Relative gene expression was determined using the $2^{-\Delta\Delta CT}$ method described by Livak and
622 Schmittgen (2001) using *UBIQUITIN-CONJUGATING ENZYME18* (*Brachypodium*
623 *distachyon*; (Hong et al., 2008); Schwartz *et al.* 2010) for normalization. All primers were

624 previously used by Ream *et al.* (2014) and had PCR efficiency ranging from 95 to 110%.
625 Statistical analysis of gene expression was performed using R (Version 3.2.3). Comparisons
626 between all genotype by treatment combinations were made with pairwise *t*-tests using log
627 transformed relative expression levels, with *p*-values corrected for multiple hypothesis testing
628 based on the Benjamini-Hochberg approach.

629

630 *Accession numbers for data in public repositories*

631 Raw resequencing reads of ABR6 have been submitted to the NCBI Short Read Archive
632 under the BioProject ID PRJNA319372 and SRA accession SRX1720894. The ABR6 *de*
633 *novo* assembly has been deposited at DDBJ/ENA/GenBank under the accession
634 LXJM00000000. The version described in this paper is version LXJM01000000. Raw
635 RNAseq reads have been submitted to the NCBI Short Read Archive under the BioProject ID
636 PRJNA319373 and SRA accessions SRX1721358 (ABR6) and SRX1721359 (Bd21).

637

638

639 **Acknowledgements**

640 We thank John Vogel for sharing preliminary sequencing data, Burkhard Steuernagel for
641 assistance with the *de novo* assembly of the ABR6 genome, David Garvin and Luis Mur for
642 providing seed, and Claire Collett, Ray Smith, Tom Thomas, and Aliyah Debbonaire for
643 assistance with population progression. MassARRAY genotyping was performed at the
644 Genomic Technologies Facility at Iowa State University. The work was funded by the
645 Biotechnology and Biological Sciences Research Council Doctoral Training Programme
646 (BB/F017294/1) and Institute Strategic Programme (BB/J004553/1), the Gatsby Charitable
647 Foundation, the Leverhulme Trust (Grant reference 10754), the 2Blades Foundation, and the
648 Human Frontiers Science Program (LT000218/2011).

649 **Tables**

650

651 **Table 1.** Significant flowering time QTLs (*qFLT*) in the different environments identified
 652 using several binary, non-parametric, and parametric approaches.

Locus	Chr^a	cM	Allele^b	E1^c	E2	E3	E4	E5
<i>qFLT1</i>	Bd1	297.6	Bd21	B, T2, T3, NP ^d	T1, T3, NP	T2, T3, NP	T2, T3	T1, T2, T3, NP
<i>qFLT2</i>	Bd1	465.2	Bd21	T2	-	-	-	-
<i>qFLT3</i>	Bd2	338.3	ABR6	-	-	-	NP	T2, T3
<i>qFLT4</i>	Bd2	409.0	Bd21	-	T1, T3	-	-	-
<i>qFLT5</i>	Bd3	60.8	Bd21	-	-	-	T1	-
<i>qFLT6</i>	Bd3	91.2	Bd21	T2, T3	T1, T3	T2, T3	-	-
<i>qFLT7</i>	Bd3	294.6	Bd21	-	-	-	T2, T3, NP	B, T2, T3, NP
<i>qFLT8</i>	Bd4	90.1	Bd21	-	-	-	NP	-

653 ^aChromosome654 ^bAllele that reduces flowering time655 ^cEnvironment (see Supplemental Table S1)

656 ^dQTL analyses were performed with interval mapping using binary classification (B) and
 657 non-parametric analysis (NP), and composite interval mapping using transformed data (T1,
 658 T2, and T3).

659 **Table 2.** Significant QTLs from composite interval mapping of transformed flowering time
 660 phenotypes (T3) in the ABR6 x Bd21 F_{4:5} families.

ENV ^a	Locus	Chr ^b	cM	EWT ^c	LOD	AEE ^d	PVE ^e	1-LOD SI ^f
1	<i>qFLT1</i>	Bd1	297.6	3.06	12.96	2.87	36.3%	296.1 - 305.6
1	<i>qFLT6</i>	Bd3	91.2	3.06	4.51	1.64	11.8%	ND
2	<i>qFLT1</i>	Bd1	297.6	3.09	7.59	0.82	20.0%	296.1 - 305.6
2	<i>qFLT4</i>	Bd2	409.0	3.09	3.20	0.47	6.7%	403.2 - 411.0
2	<i>qFLT6</i>	Bd3	93.2	3.09	6.64	0.79	18.2%	72.9 - 97.0
3	<i>qFLT1</i>	Bd1	297.6	3.20	8.61	1.50	31.1%	292.1 - 303.6
3	<i>qFLT6</i>	Bd3	91.2	3.20	5.69	1.20	18.7%	74.9 - 97.0
4	<i>qFLT1</i>	Bd1	297.6	3.19	3.49	1.77	15.9%	292.1 - 305.6
4	<i>qFLT7</i>	Bd3	294.6	3.19	3.79	1.59	14.0%	273.9 - 300.7
5	<i>qFLT1</i>	Bd1	297.6	3.17	8.62	3.43	37.5%	294.1 - 301.6
5	<i>qFLT3</i>	Bd2	338.3	3.17	3.70	-1.75	9.9%	323.7 - 348.0
5	<i>qFLT7</i>	Bd3	294.6	3.17	5.61	2.02	13.6%	275.9 - 302.0

661 ^aEnvironment (see Supplemental Table S1)

662 ^bChromosome

663 ^cExperiment-wide permutation threshold

664 ^dAdditive effect estimate for transformed phenotypes

665 ^ePercent of phenotypic variance explained

666 ^fOne-LOD support interval (cM); ND denotes QTLs not detected using standard interval
 667 mapping.

668 **Table 3.** Previously identified *B. distachyon* homologs of flowering regulators in *Arabidopsis*
 669 (*At*), hexaploid and diploid wheat (*Ta* and *Tm*), barley (*Hv*), and rice (*Os*) within the one-
 670 LOD support intervals of the statistically significant QTLs under transformation T3.

Locus	Chr^a	1-LOD SI^b	<i>B. distachyon</i> gene	Homologous genes^c
<i>qFLT1</i>	Bd1	292.1 - 305.6	Bradi1g45810	<i>AtAGL24</i> , <i>TaVRT2</i> , <i>OsMADS55</i>
			Bradi1g46060	<i>AtABF1</i>
			Bradi1g48340	<i>AtCLF</i> , <i>OsCLF</i>
			Bradi1g48830	<i>AtTSF</i> , <i>HvFT1</i> , <i>OsHd3a/OsFTL2</i>
<i>qFLT3</i>	Bd2	323.7 - 348.0	Bradi2g53060	<i>AtFDP</i>
			Bradi2g54200	<i>AtNF-YB10</i>
			Bradi2g55550	<i>AtbZIP67</i>
<i>qFLT4</i>	Bd2	403.2 - 411.0	Bradi2g60820	<i>AtFY</i> , <i>OsFY</i>
			Bradi2g62070	<i>AtLUX</i> , <i>OsLUX</i>
<i>qFLT6</i>	Bd3	72.9 - 97.0	Bradi3g08890	<i>OsFTL13</i>
			Bradi3g10010	<i>TaVRN2</i> , <i>TmCCT2</i> , <i>OsGhd7</i>
			Bradi3g12900	<i>AtHUA2</i>
<i>qFLT7</i>	Bd3	273.9 - 300.7	Bradi3g41300	<i>OsMADS37</i>
			Bradi3g42910	<i>AtSPY</i> , <i>OsSPY</i>
			Bradi3g44860	<i>OsRCN2</i>

671 ^aChromosome

672 ^bCombined maximal one-LOD support interval (cM) from all significant QTLs

673 ^cIdentified in Higgins *et al.* 2010 and Ream *et al.* 2012

674 **Figures**

675

676 **Figure 1.** Flowering behavior within the ABR6 x Bd21 mapping population. Three months
677 after a six-week vernalization period, ABR6 (left) is not flowering, whereas Bd21 (center) is
678 flowering and an individual in the ABR6 x Bd21 mapping population displays an
679 intermediate flowering phenotype (right).

680

681 **Figure 2.** Effect of vernalization on flowering time in ABR6 and Bd21. Days to flowering
682 was measured from the end of vernalization for seven different vernalization periods. After
683 vernalization plants were grown in a growth chamber (16 h photoperiod) for 35 days and then
684 transferred to a greenhouse without light and temperature control (late April to mid July
685 2013; Norwich, UK). Mean days to flowering and standard error are based on six biological
686 replicates. Different letters represent statistically significant differences based on pairwise
687 comparisons using *t*-tests with pooled standard deviations and Bonferroni correction for
688 multiple comparisons.

689

690 **Figure 3.** Segregation distortion in the ABR6 x Bd21 F₄ population. For each marker of the
691 genetic map the frequencies of F₄ individuals with homozygous ABR6 genotype (solid
692 magenta), homozygous Bd21 genotype (dashed green), or heterozygous genotype (solid
693 black) were calculated (scale on left). Data coverage (percent of F₄ individuals with genotype
694 calls per marker) is represented by the gray line (scale on right).

695

696 **Figure 4.** Frequency distribution of flowering time in the ABR6 x Bd21 population.
697 Flowering time was measured from the first day that flowering was observed in the entire
698 population. (A) Environment 1 (April to July, natural light supplemented for 20h, 22°C/20°C,
699 no vernalization), (B) Environment 2 (April to July, natural light supplemented for 20h,
700 22°C/20°C, six weeks vernalization), (C) Environment 3 (May to July, natural light and
701 temperatures, no vernalization), (D) Environment 4 (September to November, natural light
702 supplemented for 16h, minimum 18°C/11.5°C, no vernalization), (E) Environment 5 (March
703 to May, natural light and temperatures, no vernalization). Flowering times for the parental
704 lines are indicated by arrows (no data for Environment 3). NF = not flowering.

705

706 **Figure 5.** Linkage mapping of flowering time in the ABR6 x Bd21 population. Time to
707 flowering for 114 F_{4.5} families of the population was transformed into ordered rank values,

708 QTL analysis performed using composite interval mapping under an additive model
709 hypothesis test ($H_0:H_1$), and plotted based on normalized permutation thresholds. The blue
710 horizontal line represents the threshold of statistical significance based on 1,000
711 permutations. Orange = Environment 1(April to July, natural light supplemented for 20h,
712 22°C/20°C, no vernalization), blue = Environment 2 (April to July, natural light
713 supplemented for 20h, 22°C/20°C, six weeks vernalization), red = Environment 3 (May to
714 July, natural light and temperatures, no vernalization), yellow = Environment 4 (September to
715 November, natural light supplemented for 16h, minimum 18°C/11.5°C, no vernalization),
716 green = Environment 5 (March to May, natural light and temperatures, no vernalization). See
717 Supplemental Table S1 for full environmental details. The genetic positions of the previously
718 identified homologs of *VRN1*, *VRN2*, and *FT* are indicated (compare Higgins *et al.* 2010 and
719 Ream *et al.* 2012).

720

721 **Figure 6.** Phenotype by genotype plot for the two major loci controlling flowering time in the
722 ABR6 x Bd21 mapping population. Days to flowering in Environment 3 for the ABR6 x
723 Bd21 $F_{4,5}$ families homozygous at *qFLT1* and *qFLT6* shows that the Bd21 alleles at these two
724 loci promote early flowering. Error bars represent one standard error; NF = not flowering.

725

726 **Figure 7.** Comparison of the flowering regulators *FT* and *VRN2* between the *B. distachyon*
727 accessions Bd21 and ABR6. Contigs of the ABR6 *de novo* assembly were aligned to the
728 Bd21 reference sequence (Version 3) and polymorphisms were identified in the genes of
729 interest and 2kb promoter and terminator sequence (1.9kb promoter for *VRN2*). Red ticks
730 represent SNPs and black ticks represent indels. The length of indels (bp) is shown with + for
731 insertion and – for deletion. The amino acid change of the non-synonymous SNP in *VRN2* is
732 indicated. s = synonymous SNP; dashed line = promoter or terminator; white box = 5'-UTR
733 or 3'-UTR; black box = exon; black line = intron; M = methionine/translation start; star =
734 translation stop; black bar under *VRN2* = CCT domain.

735

736 **Figure 8.** *VRN1*, *VRN2*, and *FT* expression in fourth leaf of ABR6 and Bd21 after varying
737 periods of cold treatment. Seeds were imbibed with water and not vernalized or vernalized
738 for two, four, or six weeks, and transferred to a growth chamber with parameters similar to
739 Environment 2. Fully expanded fourth leaves were harvested in the middle of the
740 photoperiod. Relative gene expression of *VRN1* (A), *VRN2* (B), and *FT* (C) was determined
741 using RT-qPCR and analyzed using the $2^{-\Delta\Delta Ct}$ method. All genes were normalized to 1
based

742 on Bd21 expression with no cold treatment (0 weeks) and *UBQ18* was used as internal
743 control. Bars represent the mean of three biological replicates with error bars showing ± 1
744 standard error. Different letters represent statistically significant differences based on
745 pairwise *t*-tests using a multiple hypothesis corrected *p*-value threshold of 0.05 with the
746 Benjamini-Hochberg approach.

747 **Supplemental Material**

748

749 **Supplemental Figure S1.** Linkage groups of ABR6 x Bd21 genetic map.

750 **Supplemental Figure S2.** Two-way recombination fraction plot for the ABR6 x Bd21 F₄
751 population.

752 **Supplemental Table S1.** Summary of the environmental conditions tested.

753 **Supplemental Table S2.** Significant QTLs from interval mapping of binary classification of
754 flowering time phenotypes in the ABR6 x Bd21 F_{4.5} families.

755 **Supplemental Table S3.** Significant QTLs from interval mapping using a non-parametric
756 model for flowering time phenotypes in the ABR6 x Bd21 F_{4.5} families (NP).

757 **Supplemental Table S4.** Significant QTLs from composite interval mapping of transformed
758 flowering time phenotypes in the ABR6 x Bd21 F_{4.5} families (T1).

759 **Supplemental Table S5.** Significant QTLs from composite interval mapping of transformed
760 flowering time phenotypes in the ABR6 x Bd21 F_{4.5} families (T2).

761 **Supplemental Table S6.** Summary of the structural variation between Bd21 and ABR6 for
762 the flowering regulators Bradi1g48830 (*FT*), Bradi3g10010 (*VRN2*), and Bradi1g08340
763 (*VRN1*).

764 **Supplemental Table S7.** Five cleaved amplified polymorphic sequences (CAPS) markers
765 included in the ABR6 x Bd21 genetic map design.

766 **Supplemental Data S1.** Raw, binary, and transformed flowering time data for the ABR6 x
767 Bd21 F_{4.5} families in the five environments tested.

768 **Supplemental Data S2.** Sequence information used to develop iPLEX assays for the
769 MassARRAY markers in the ABR6 x Bd21 genetic map design.

770 **Supplemental Data S3.** ABR6 x Bd21 genetic map.

771

772

773 **Supplemental Figure S1.** Linkage groups of ABR6 x Bd21 genetic map. Cumulative cM
774 distances and SNP marker names are shown to the left and right of each chromosome,
775 respectively. cM distance at the F₄ stage was estimated using the Kosambi function. SNP
776 marker names consist of the corresponding chromosome and physical position in the Bd21
777 reference genome (Version 3).

778

779 **Supplemental Figure S2.** Two-way recombination fraction plot for the ABR6 x Bd21 F₄
780 population.

781

782 **Supplemental Table S1.** Summary of the environmental conditions tested.

783

784 **Supplemental Table S2.** Significant QTLs from interval mapping of binary classification of
785 flowering time phenotypes in the ABR6 x Bd21 F_{4:5} families.

786

787 **Supplemental Table S3.** Significant QTLs from interval mapping using a non-parametric
788 model for flowering time phenotypes in the ABR6 x Bd21 F_{4:5} families (NP).

789

790 **Supplemental Table S4.** Significant QTLs from composite interval mapping of transformed
791 flowering time phenotypes in the ABR6 x Bd21 F_{4:5} families (T1).

792

793 **Supplemental Table S5.** Significant QTLs from composite interval mapping of transformed
794 flowering time phenotypes in the ABR6 x Bd21 F_{4:5} families (T2).

795

796 **Supplemental Table S6.** Summary of the structural variation between Bd21 and ABR6 for
797 the flowering regulators Bradi1g48830 (*FT*), Bradi3g10010 (*VRN2*), and Bradi1g08340
798 (*VRN1*).

799

800 **Supplemental Table S7.** Five cleaved amplified polymorphic sequences (CAPS) markers
801 included in the ABR6 x Bd21 genetic map design. Marker names consist of the
802 corresponding chromosome and physical position in the Bd21 reference genome (Version 3).
803 Synonymous names refer to Barbieri *et al.* 2012.

804

805 **Supplemental Data S1.** Raw, binary, and transformed flowering time data for the ABR6 x
806 Bd21 F_{4:5} families in the five environments tested.

807

808 **Supplemental Data S2.** Sequence information used to develop iPLEX assays for the 247
809 MassARRAY markers in the ABR6 x Bd21 genetic map design. Marker names consist of the
810 corresponding chromosome and physical position in the Bd21 reference genome (Version 3)
811 and SNPs are indicated in square brackets.

812

813 **Supplemental Data S3.** ABR6 x Bd21 genetic map. “A” genotype calls refer to ABR6, “B”
814 genotype calls to Bd21, “H” genotype calls to heterozygous markers and “-“ to missing data
815 points.

Parsed Citations

Amasino R (2010) Seasonal and developmental timing of flowering. *Plant J* 61: 1001-1013

Pubmed: [Author and Title](#)

CrossRef: [Author and Title](#)

Google Scholar: [Author Only Title Only Author and Title](#)

Andrés F, Coupland G (2012) The genetic basis of flowering responses to seasonal cues. *Nat Rev Genet* 13: 627-639

Pubmed: [Author and Title](#)

CrossRef: [Author and Title](#)

Google Scholar: [Author Only Title Only Author and Title](#)

Barbieri M, Marcel TC, Niks RE, Francia E, Pasquariello M, Mazzamurro V, Garvin DF, Pecchioni N (2012) QTLs for resistance to the false brome rust *Puccinia brachypodii* in the model grass *Brachypodium distachyon* L. *Genome* 55: 152-163

Pubmed: [Author and Title](#)

CrossRef: [Author and Title](#)

Google Scholar: [Author Only Title Only Author and Title](#)

Basten CJ, Weir BS, Zeng Z-B (2004) QTL Cartographer, version 1.17. Department of Statistics, North Carolina State University, Raleigh, NC

Pubmed: [Author and Title](#)

CrossRef: [Author and Title](#)

Google Scholar: [Author Only Title Only Author and Title](#)

Bolger AM, Lohse M, Usadel B (2014) Trimmomatic: a flexible trimmer for Illumina sequence data. *Bioinformatics* 30: 2114-2120

Pubmed: [Author and Title](#)

CrossRef: [Author and Title](#)

Google Scholar: [Author Only Title Only Author and Title](#)

Bombliès K, Lempe J, Epple P, Warthmann N, Lanz C, Dangl JL, Weigel D (2007) Autoimmune response as a mechanism for a Dobzhansky-Muller-type incompatibility syndrome in plants. *PLoS Biology* 5: e236

Pubmed: [Author and Title](#)

CrossRef: [Author and Title](#)

Google Scholar: [Author Only Title Only Author and Title](#)

Bombliès K, Weigel D (2007) Hybrid necrosis: autoimmunity as a potential gene-flow barrier in plant species. *Nat Rev Genet* 8: 382-393

Pubmed: [Author and Title](#)

CrossRef: [Author and Title](#)

Google Scholar: [Author Only Title Only Author and Title](#)

Broman KW, Sen S, Owens SE, Manichaikul A, Southard-Smith EM, Churchill GA (2006) The X chromosome in quantitative trait locus mapping. *Genetics* 174: 2151-2158

Pubmed: [Author and Title](#)

CrossRef: [Author and Title](#)

Google Scholar: [Author Only Title Only Author and Title](#)

Broman KW, Wu H, Sen S, Churchill GA (2003) R/qtl: QTL mapping in experimental crosses. *Bioinformatics* 19: 889-890

Pubmed: [Author and Title](#)

CrossRef: [Author and Title](#)

Google Scholar: [Author Only Title Only Author and Title](#)

Catalán P, Chalhoub B, Chochois V, Garvin DF, Hasterok R, Manzaneda AJ, Mur LA, Pecchioni N, Rasmussen SK, Vogel JP, Voxeur A (2014) Update on the genomics and basic biology of *Brachypodium*: International *Brachypodium Initiative* (IBI). *Trends Plant Sci* 19: 414-418

Pubmed: [Author and Title](#)

CrossRef: [Author and Title](#)

Google Scholar: [Author Only Title Only Author and Title](#)

Chen A, Dubcovsky J (2012) Wheat TILLING mutants show that the vernalization gene *VRN1* down-regulates the flowering repressor *VRN2* in leaves but is not essential for flowering. *PLoS Genet* 8: e1003134

Pubmed: [Author and Title](#)

CrossRef: [Author and Title](#)

Google Scholar: [Author Only Title Only Author and Title](#)

Dawson AM, Bettgenhaeuser J, Gardiner M, Green P, Hernández-Pinzón I, Hubbard A, Moscou MJ (2015) The development of quick, robust, quantitative phenotypic assays for describing the host-nonhost landscape to stripe rust. *Frontiers in Plant Science* 6

Pubmed: [Author and Title](#)

CrossRef: [Author and Title](#)

Google Scholar: [Author Only Title Only Author and Title](#)

Dawson AM, Ferguson JN, Gardiner M, Green P, Hubbard A, Moscou MJ (2016) Isolation and fine mapping of *Rps6*: an intermediate host resistance gene in barley to wheat stripe rust. *Theoretical and Applied Genetics* 129: 831-843

Pubmed: [Author and Title](#)

CrossRef: [Author and Title](#)

Google Scholar: [Author Only Title Only Author and Title](#)

Distelfeld A, Li C, Dubcovsky J (2009) Regulation of flowering in temperate cereals. *Curr Opin Plant Biol* 12: 178-184

Pubmed: [Author and Title](#) Downloaded from www.plantphysiol.org on September 20, 2016 - Published by www.plantphysiol.org

CrossRef: [Author and Title](#)
Google Scholar: [Author Only Title Only Author and Title](#)

Doerge RW, Churchill GA(1996) Permutation tests for multiple loci affecting a quantitative character. Genetics 142: 285-294

Pubmed: [Author and Title](#)
CrossRef: [Author and Title](#)
Google Scholar: [Author Only Title Only Author and Title](#)

Draper J, Mur LA, Jenkins G, Ghosh-Biswas GC, Bablak P, Hasterok R, Routledge AP(2001) Brachypodium distachyon. A new model system for functional genomics in grasses. Plant Physiol 127: 1539-1555

Pubmed: [Author and Title](#)
CrossRef: [Author and Title](#)
Google Scholar: [Author Only Title Only Author and Title](#)

Dubcovsky J, Chen C, Yan L (2005) Molecular characterization of the allelic variation at the VRN-H2 vernalization locus in barley. Molecular Breeding 15: 395-407

Pubmed: [Author and Title](#)
CrossRef: [Author and Title](#)
Google Scholar: [Author Only Title Only Author and Title](#)

Faris JD, Laddomada B, Gill BS (1998) Molecular mapping of segregation distortion loci in Aegilops tauschii. Genetics 149: 319-327

Pubmed: [Author and Title](#)
CrossRef: [Author and Title](#)
Google Scholar: [Author Only Title Only Author and Title](#)

Fu D, Szücs P, Yan L, Helguera M, Skinner JS, von Zitzewitz J, Hayes PM, Dubcovsky J (2005) Large deletions within the first intron in VRN-1 are associated with spring growth habit in barley and wheat. Mol Genet Genomics 273: 54-65

Pubmed: [Author and Title](#)
CrossRef: [Author and Title](#)
Google Scholar: [Author Only Title Only Author and Title](#)

Garvin DF, Gu Y-Q, Hasterok R, Hazen SP, Jenkins G, Mockler TC, Mur LAJ, Vogel JP (2008) Development of genetic and genomic research resources for Brachypodium distachyon, a new model system for grass crop research. Crop Science 48: S-69

Pubmed: [Author and Title](#)
CrossRef: [Author and Title](#)
Google Scholar: [Author Only Title Only Author and Title](#)

Higgins JA, Bailey PC, Laurie DA(2010) Comparative genomics of flowering time pathways using Brachypodium distachyon as a model for the temperate grasses. PLoS One 5: e10065

Pubmed: [Author and Title](#)
CrossRef: [Author and Title](#)
Google Scholar: [Author Only Title Only Author and Title](#)

Hong SY, Seo PJ, Yang MS, Xiang F, Park CM (2008) Exploring valid reference genes for gene expression studies in Brachypodium distachyon by real-time PCR. BMC Plant Biol 8: 112

Pubmed: [Author and Title](#)
CrossRef: [Author and Title](#)
Google Scholar: [Author Only Title Only Author and Title](#)

Huo N, Garvin DF, You FM, McMahon S, Luo MC, Gu YQ, Lazo GR, Vogel JP (2011) Comparison of a high-density genetic linkage map to genome features in the model grass Brachypodium distachyon. Theor Appl Genet 123: 455-464

Pubmed: [Author and Title](#)
CrossRef: [Author and Title](#)
Google Scholar: [Author Only Title Only Author and Title](#)

Jung C, Müller AE (2009) Flowering time control and applications in plant breeding. Trends Plant Sci 14: 563-573

Pubmed: [Author and Title](#)
CrossRef: [Author and Title](#)
Google Scholar: [Author Only Title Only Author and Title](#)

Kardailskiy I, Shukla VK, Ahn JH, Dagenais N, Christensen SK, Nguyen JT, Chory J, Harrison MJ, Weigel D (1999) Activation tagging of the floral inducer FT. Science 286: 1962-1965

Pubmed: [Author and Title](#)
CrossRef: [Author and Title](#)
Google Scholar: [Author Only Title Only Author and Title](#)

Karsai I, Szücs P, Mészáros K, Filichkina T, Hayes PM, Skinner JS, Lang L, Bedö Z (2005) The Vrn-H2 locus is a major determinant of flowering time in a facultative x winter growth habit barley (Hordeum vulgare L.) mapping population. Theoretical and Applied Genetics 110: 1458-1466

Pubmed: [Author and Title](#)
CrossRef: [Author and Title](#)
Google Scholar: [Author Only Title Only Author and Title](#)

Koboldt DC, Chen K, Wylie T, Larson DE, McLellan MD, Mardis ER, Weinstock GM, Wilson RK, Ding L (2009) VarScan: variant detection in massively parallel sequencing of individual and pooled samples. Bioinformatics 25: 2283-2285

Pubmed: [Author and Title](#)
CrossRef: [Author and Title](#)
Google Scholar: [Author Only Title Only Author and Title](#)

Konieczny A, Ausubel FM (1993) A procedure for mapping Arabidopsis mutations using co-dominant ecotype-specific PCR-based markers. The Plant Journal

Pubmed: [Author and Title](#)

CrossRef: [Author and Title](#)

Google Scholar: [Author Only Title Only Author and Title](#)

Koornneef M, Alonso-Blanco C, Vreugdenhil D (2004) Naturally occurring genetic variation in Arabidopsis thaliana. Annu Rev Plant Biol 55: 141-172

Pubmed: [Author and Title](#)

CrossRef: [Author and Title](#)

Google Scholar: [Author Only Title Only Author and Title](#)

Kruglyak L, Lander ES (1995) Anonparametric approach for mapping quantitative trait loci. Genetics 139: 1421-1428

Pubmed: [Author and Title](#)

CrossRef: [Author and Title](#)

Google Scholar: [Author Only Title Only Author and Title](#)

Lander ES, Botstein D (1989) Mapping mendelian factors underlying quantitative traits using RFLP linkage maps. Genetics 121: 185-199

Pubmed: [Author and Title](#)

CrossRef: [Author and Title](#)

Google Scholar: [Author Only Title Only Author and Title](#)

Lauter N, Moscou MJ, Habiger J, Moose SP (2008) Quantitative genetic dissection of shoot architecture traits in maize: towards a functional genomics approach. The Plant Genome 1: 99

Pubmed: [Author and Title](#)

CrossRef: [Author and Title](#)

Google Scholar: [Author Only Title Only Author and Title](#)

Li H, Durbin R (2009) Fast and accurate short read alignment with Burrows-Wheeler transform. Bioinformatics 25: 1754-1760

Pubmed: [Author and Title](#)

CrossRef: [Author and Title](#)

Google Scholar: [Author Only Title Only Author and Title](#)

Livak KJ, Schmittgen TD (2001) Analysis of relative gene expression data using real-time quantitative PCR and the 2⁻(Delta Delta C(T)) method. Methods 25: 402-408

Pubmed: [Author and Title](#)

CrossRef: [Author and Title](#)

Google Scholar: [Author Only Title Only Author and Title](#)

Lu H, Romero-Severson J, Bernardo R (2002) Chromosomal regions associated with segregation distortion in maize. Theor Appl Genet 105: 622-628

Pubmed: [Author and Title](#)

CrossRef: [Author and Title](#)

Google Scholar: [Author Only Title Only Author and Title](#)

Lv B, Nitcher R, Han X, Wang S, Ni F, Li K, Pearce S, Wu J, Dubcovsky J, Fu D (2014) Characterization of FLOWERING LOCUS T1 (FT1) gene in Brachypodium and wheat. PLoS One 9: e94171

Pubmed: [Author and Title](#)

CrossRef: [Author and Title](#)

Google Scholar: [Author Only Title Only Author and Title](#)

Manly KF, Cudmore RH, Meer JM (2014) Map Manager QTX, cross-platform software for genetic mapping. Mammalian Genome 12: 930-932

Pubmed: [Author and Title](#)

CrossRef: [Author and Title](#)

Google Scholar: [Author Only Title Only Author and Title](#)

Muñoz-Amatrián M, Moscou MJ, Bhat PR, Svensson JT, Bartos? J, Suchánková P, S?imkova´ H, Endo TR, Fenton RD, Lonardi S, Castillo AM, Chao SM, Cistué L, Cuesta-Marcos A, Forrest KL, Hayden MJ, Hayes PM, Horsley RD, Makoto K, Moody D, Sato K, Vallés MP, Wulff BBH, Muehlbauer GJ, Dolez?el J, Close TJ (2011) An improved consensus linkage map of barley based on flow-sorted chromosomes and single nucleotide polymorphism markers. Plant Genome 4: 238-249

Pubmed: [Author and Title](#)

CrossRef: [Author and Title](#)

Google Scholar: [Author Only Title Only Author and Title](#)

Opanowicz M, Vain P, Draper J, Parker D, Doonan JH (2008) Brachypodium distachyon: making hay with a wild grass. Trends Plant Sci 13: 172-177

Pubmed: [Author and Title](#)

CrossRef: [Author and Title](#)

Google Scholar: [Author Only Title Only Author and Title](#)

Ream TS, Woods DP, Amasino RM (2012) The molecular basis of vernalization in different plant groups. Cold Spring Harbor Symposia on Quantitative Biology 77: 105-115

Pubmed: [Author and Title](#)

CrossRef: [Author and Title](#)

Google Scholar: [Author Only Title Only Author and Title](#)

Ream TS, Woods DP, Schwartz CJ, Sanabria CP, Mahoy JA, Walters EM, Kaeppler HF, Amasino RM (2014) Interaction of photoperiod and vernalization determines flowering time of Brachypodium distachyon. Plant Physiol 164: 694-709

Pubmed: [Author and Title](#)

CrossRef: [Author and Title](#)

Routledge APM, Shelley G, Smith JV, Talbot NJ, Draper J, Mur LAJ (2004) Magnaporthe grisea interactions with the model grass Brachypodium distachyon closely resemble those with rice (Oryza sativa). Molecular Plant Pathology 5: 253-265

Pubmed: [Author and Title](#)

CrossRef: [Author and Title](#)

Google Scholar: [Author Only Title Only Author and Title](#)

Royston JP (1982) An Extension of Shapiro and Wilk's W Test for Normality to Large Samples. Applied Statistics 31: 115

Pubmed: [Author and Title](#)

CrossRef: [Author and Title](#)

Google Scholar: [Author Only Title Only Author and Title](#)

Sasani S, Hemming MN, Oliver SN, Greenup A, Tavakkol-Afshari R, Mahfoozi S, Poustini K, Sharifi HR, Dennis ES, Peacock WJ, Trevaskis B (2009) The influence of vernalization and daylength on expression of flowering-time genes in the shoot apex and leaves of barley (Hordeum vulgare). J Exp Bot 60: 2169-2178

Pubmed: [Author and Title](#)

CrossRef: [Author and Title](#)

Google Scholar: [Author Only Title Only Author and Title](#)

Schwartz CJ, Doyle MR, Manzaneda AJ, Rey PJ, Mitchell-Olds T, Amasino RM (2010) Natural variation of flowering time and vernalization responsiveness in Brachypodium distachyon. BioEnergy Research 3: 38-46

Pubmed: [Author and Title](#)

CrossRef: [Author and Title](#)

Google Scholar: [Author Only Title Only Author and Title](#)

Tan S, Wu S (2012) Genome wide analysis of nucleotide-binding site disease resistance genes in Brachypodium distachyon. Comp Funct Genomics 2012: 418208

Pubmed: [Author and Title](#)

CrossRef: [Author and Title](#)

Google Scholar: [Author Only Title Only Author and Title](#)

The International Brachypodium Initiative (2010) Genome sequencing and analysis of the model grass Brachypodium distachyon. Nature 463: 763-768

Pubmed: [Author and Title](#)

CrossRef: [Author and Title](#)

Google Scholar: [Author Only Title Only Author and Title](#)

Trapnell C, Pachter L, Salzberg SL (2009) TopHat: discovering splice junctions with RNA-Seq. Bioinformatics 25: 1105-1111

Pubmed: [Author and Title](#)

CrossRef: [Author and Title](#)

Google Scholar: [Author Only Title Only Author and Title](#)

Tyler L, Lee SJ, Young ND, Delulio GA, Benavente E, Reagon M, Sysopha J, Baldini RM, Troi`a A, Hazen SP, Caicedo AL (2016) Population structure in the model grass Brachypodium distachyon is highly correlated with flowering differences across broad geographic areas. The Plant Genome 9: 1-20

Pubmed: [Author and Title](#)

CrossRef: [Author and Title](#)

Google Scholar: [Author Only Title Only Author and Title](#)

Vain P, Worland B, Thole V, McKenzie N, Alves SC, Opanowicz M, Fish LJ, Bevan MW, Snape JW (2008) Agrobacterium-mediated transformation of the temperate grass Brachypodium distachyon (genotype Bd21) for T-DNA insertional mutagenesis. Plant Biotechnol J 6: 236-245

Pubmed: [Author and Title](#)

CrossRef: [Author and Title](#)

Google Scholar: [Author Only Title Only Author and Title](#)

Vogel JP, Garvin DF, Leong OM, Hayden DM (2006) Agrobacterium-mediated transformation and inbred line development in the model grass Brachypodium distachyon. Plant Cell, Tissue and Organ Culture 84: 199-211

Pubmed: [Author and Title](#)

CrossRef: [Author and Title](#)

Google Scholar: [Author Only Title Only Author and Title](#)

von Zitzewitz J, Szücs P, Dubcovsky J, Yan L, Francia E, Pecchioni N, Casas A, Chen TH, Hayes PM, Skinner JS (2005) Molecular and structural characterization of barley vernalization genes. Plant Mol Biol 59: 449-467

Pubmed: [Author and Title](#)

CrossRef: [Author and Title](#)

Google Scholar: [Author Only Title Only Author and Title](#)

Wilczek AM, Burghardt LT, Cobb AR, Cooper MD, Welch SM, Schmitt J (2010) Genetic and physiological bases for phenological responses to current and predicted climates. Philosophical Transactions of the Royal Society of London, Series B: Biological Sciences 365: 3129-3147

Pubmed: [Author and Title](#)

CrossRef: [Author and Title](#)

Google Scholar: [Author Only Title Only Author and Title](#)

Wilson P, Streich J, Borevitz J (2016) Genomic diversity and climate adaptation in Brachypodium. In JP Vogel, ed, Genetics and Genomics of Brachypodium. Springer International Publishing, pp 107-127

Pubmed: [Author and Title](#)

CrossRef: [Author and Title](#)

Google Scholar: [Author Only Title Only Author and Title](#)

Woods D, Amasino R (2016) Dissecting the control of flowering time in grasses using *Brachypodium distachyon*. In JP Vogel, ed, *Genetics and Genomics of Brachypodium*. Springer International Publishing, pp 259-273

Pubmed: [Author and Title](#)

CrossRef: [Author and Title](#)

Google Scholar: [Author Only Title Only Author and Title](#)

Woods D, Bednarek R, Bouché F, Gordon SP, Vogel J, Garvin DF, Amasino R (2016) Genetic architecture of flowering-time variation in *Brachypodium distachyon*.

Woods D, McKeown M, Dong Y, Preston JC, Amasino RM (2016) Evolution of VRN2/GhD7-like genes in vernalization-mediated repression of grass flowering. *Plant Physiol*

Pubmed: [Author and Title](#)

CrossRef: [Author and Title](#)

Google Scholar: [Author Only Title Only Author and Title](#)

Woods DP, Ream TS, Minevich G, Hobert O, Amasino RM (2014) PHYTOCHROME C is an essential light receptor for photoperiodic flowering in the temperate grass, *Brachypodium distachyon*. *Genetics* 198:397-408

Pubmed: [Author and Title](#)

CrossRef: [Author and Title](#)

Google Scholar: [Author Only Title Only Author and Title](#)

Xu SZ, Atchley WR (1996) Mapping quantitative trait loci for complex binary diseases using line crosses. *Genetics* 143:1417-1424

Pubmed: [Author and Title](#)

CrossRef: [Author and Title](#)

Google Scholar: [Author Only Title Only Author and Title](#)

Xu Y, Zhu L, Xiao J, Huang N, McCouch SR (1997) Chromosomal regions associated with segregation distortion of molecular markers in F₂, backcross, doubled haploid, and recombinant inbred populations in rice (*Oryza sativa* L). *Molecular and General Genetics* 253: 535-545

Pubmed: [Author and Title](#)

CrossRef: [Author and Title](#)

Google Scholar: [Author Only Title Only Author and Title](#)

Yan L, Fu D, Li C, Blechl A, Tranquilli G, Bonafede M, Sanchez A, Valarik M, Yasuda S, Dubcovsky J (2006) The wheat and barley vernalization gene VRN3 is an orthologue of FT. *Proceedings of the National Academy of Sciences, USA* 103:19581-19586

Pubmed: [Author and Title](#)

CrossRef: [Author and Title](#)

Google Scholar: [Author Only Title Only Author and Title](#)

Yan L, Loukoianov A, Blechl A, Tranquilli G, Ramakrishna W, SanMiguel P, Bennetzen JL, Echenique V, Dubcovsky J (2004) The wheat VRN2 gene is a flowering repressor down-regulated by vernalization. *Science* 303:1640-1644

Pubmed: [Author and Title](#)

CrossRef: [Author and Title](#)

Google Scholar: [Author Only Title Only Author and Title](#)

Yan L, Loukoianov A, Tranquilli G, Helguera M, Fahima T, Dubcovsky J (2003) Positional cloning of the wheat vernalization gene VRN1. *Proceedings of the National Academy of Sciences, USA* 100:6263-6268

Pubmed: [Author and Title](#)

CrossRef: [Author and Title](#)

Google Scholar: [Author Only Title Only Author and Title](#)

Zeng Z-B (1993) Theoretical basis for separation of multiple linked gene effects in mapping quantitative trait loci. *Proceedings of the National Academy of Sciences, USA* 90:10972-10976

Pubmed: [Author and Title](#)

CrossRef: [Author and Title](#)

Google Scholar: [Author Only Title Only Author and Title](#)

Zeng Z-B (1994) Precision mapping of quantitative trait loci. *Genetics* 136: 1457-1468

Pubmed: [Author and Title](#)

CrossRef: [Author and Title](#)

Google Scholar: [Author Only Title Only Author and Title](#)